Article

Not peer-reviewed version

New Benzofuran-Pyrazole Based Compounds as Promising Antimicrobial Agents: Design, Synthesis, Antioxidant, Anti-Inflammatory, DNA Gyrase B Inhibition and In Silico Studies

Somaia S. Abd El-Karim , Manal M. Anwar , Yasmin M. Syam , Hassan M. Awad , Asmaa Negm El-Dein , Mohamed K. El-Ashrey , Hamad M. Alkahtani , Sameh H Abdelwahed *

Posted Date: 24 October 2024

doi: 10.20944/preprints202408.1792.v2

Keywords: Benzofuran-pyrazole scaffold; antimicrobial activity; antioxidant; in vitro anti-inflammatory DNA gyrase enzyme; computational studies

Article

New Benzofuran-Pyrazole Based Compounds as Promising Antimicrobial Agents: Design, Synthesis, Antioxidant, Anti-Inflammatory, DNA Gyrase B Inhibition and In Silico Studies

Somaia S. Abd El-Karim [1], Manal M. Anwar [1], Yasmin M. Syam [1], Hassan M. Awad [2], Asmaa Negm El-Dein [2], Mohamed K. El-Ashrey [3,4], Hamad M. Alkahtani [5] and Sameh H. Abdelwahed [6,7,*]

[1] Department of Therapeutic Chemistry, Pharmaceutical and Drug Industries Research Institute, National Research Centre, Dokki, Cairo, P.O. 12622, Egypt; ssabdelkarim@gmail.com, manal.hasan52@live.com, ym.syam@nrc.sci.eg

[2] Chemistry of Natural and Microbial Products Department, Pharmaceutical and Drug Industries Research Institute, National Research Centre, Dokki, Cairo, P.O. 12622, Egypt; awadmmhassan@gmail.com, asmaanegm_084@yahoo.com

[3] Pharmaceutical Chemistry Department, Faculty of Pharmacy, Cairo University, Kasr Elini St., Cairo 11562, Egypt; mohamed.elashrey@pharma.cu.edu.eg

[4] Medicinal Chemistry Department, Faculty of Pharmacy, King Salman International University (KSIU), South Sinai 46612, Egypt.

[5] Department of Pharmaceutical Chemistry, College of Pharmacy, King Saud University, P.O. Box 2457, Riyadh 11451, Saudi Arabia, ahamad@ksu.edu.sa

[6] Department of Chemistry, Prairie View A&M University, Prairie View, TX 77446, USA.

[7] Department of Chemistry, Texas A&M University, College Station, TX 77843, USA

* Correspondence: shabdelwahed@pvamu.edu

Abstract: The alarming rise of antibiotic resistance has made it imperative to find novel antimicrobial medications. This study reports the design and synthesis of new molecules based on benzofuran-pyrazole scaffolds hybridized with various N/O heterocycles using the molecular hybridization process. The newly synthesized candidates were confirmed using micro-analytical and spectral analyses, and their antimicrobial characteristics were assessed against different bacterial and fungal isolates in comparison with novobiocin and clotrimazole as antibacterial and antifungal standards, respectively. In addition, the new compounds were further evaluated as *in vitro* antioxidants and anti-inflammatory congeners. The most promising broad spectrum antimicrobial compounds **9**, **10** with values ranging from 2.50-20.60 µg/mL were further examined as *E. coli* DNA gyrase B enzyme suppressors using novobiocin as a reference drug. *In silico* computational and ADMET studies were carried out for the most active compounds.

Keywords: Benzofuran-pyrazole scaffold; antimicrobial activity; antioxidant; in vitro anti-inflammatory DNA gyrase enzyme; computational studies

1. Introduction

Bacterial diseases are considered a global threat due to the fact that many bacterial isolates are increasing resistance to many antibiotics. Approximately 700,000 individuals worldwide pass away from incurable illnesses each year [1, 2].

Experts predict that if we don't solve the issue of multiple antibiotic resistance by 2050, it will claim the lives of over 10 million people worldwide. Different pathogenic microbes, such as viruses, yeasts, bacteria, and fungi, are frequently the cause of severe infections, which significantly exacerbate suffering in those with weakened immune systems and cause severe morbidity and

 doi:10.20944/preprints202408.1792.v2

mortality [3–5]. Antibiotics are effective tools in the fight against pathogenic bacteria by killing or suppressing their growth, but their misuse contributes to the emergence of antibiotic resistance, which has detrimental effects on human health [6]. The emergence and wide-spread distribution of drug-resistant bacteria including multi-drug resistant (MDR) and pan-drug resistant pathogens represent the need of the hour to develop new drugs active against both drug-sensitive and -resistant Gram-positive and Gram-negative pathogens [7-9].

Heterocyclic ring systems are powerful backbones with many biological characteristics due to their similarities to various natural bioactive molecules [10]. Benzofuran is a fundamental structural unit in a variety of biologically active natural and synthesized products [11], covering a wide range of categories such as antiviral, antibacterial, antifungal, antiparasitic, anti-TB, anticancer, anti-Alzheimer's disease, analgesic, anti-inflammatory, and antihyperglycemic activities [12–19].

Recently, numerous derivatives bearing benzofuran nucleus hybridized with different heterocyclic cores have been designed, synthesized and tested for their anti-microbial activities, and some of them showed promising potency against a panel of Gram-positive, Gram-negative and fungal strains [20-27].

In medicinal chemistry, the pyrazole ring structure is extensively spotted as a pharmacophore, and the fortification of the modern organic synthesis toolbox demands synthetic tactics to generate its derivatives. Considering the wide range of biological activities of pyrazoles and their presence in naturally occurring compounds, pyrazole has been the topic of research for thousands of researchers all over the world [28-31]. Many studies have focused on the antibacterial action of various pyrazole-based derivatives against drug-resistant bacteria and fungi owing to their interactions with DNA, enzymes, and receptors [32].

In recent studies, the hybridization of benzofuran ring with pyrazole nucleus has been identified as medically promising agents and constitutes an important scaffold in the field of designing and synthesis of promising antimicrobial, antioxidants, and anti-inflammatory candidates. Numerous benzofuran-pyrazole-based derivatives possess an excellent efficacy as antimicrobial agents. **Figure 1** represents various derivatives which are based on benzofuran-pyrazole and/or benzofuran-pyrazoline scaffolds possessing significant antimicrobial antioxidants, and anti-inflammatory activities [33-40].

Preprints.org (www.preprints.org) | NOT PEER-REVIEWED | Posted: 24 October 2024 doi:10.20944/preprints202408.1792.v2

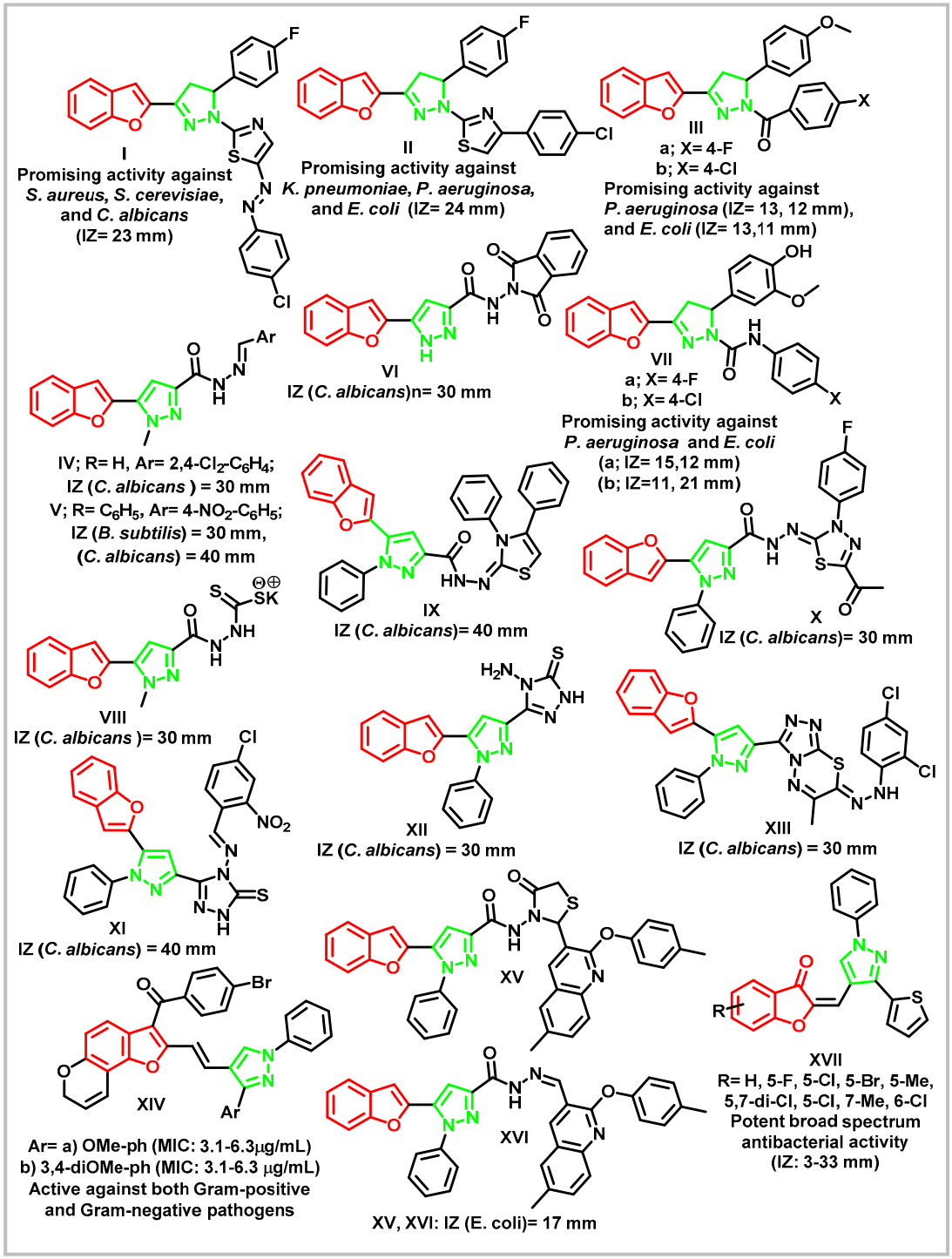

Figure 1. Examples of different molecules bearing benzofuran-pyrazole/pyrazoline scaffolds conjugated with heterocyclic rings possessing significant antimicrobial activities.

The topoisomerase enzyme is divided into three types in prokaryotic cells: type I, type II, and type III; in eukaryotes, type III is absent [41]. Type II has been divided into DNA gyrase (Gyrase A (GyrA) and B (GyrB), the two subunits of heterotetrameric DNA gyrase), and Topoisomerase IV [42]. Multiple studies have focused on Type II subunits due to their specificity in the operation of bacterial reproduction. The tyrosine residue in the GyrA subunit is considered the active site amino acid, which is important for releasing the twist in the DNA (negative supercoiling) as well as reunion (positive supercoiling), whereas the GyrB subunit has an active site that is responsible for ATPase potency, providing energy for the DNA supercoiling.

 doi:10.20944/preprints202408.1792.v2

DNA gyrase plays a unique function since it depends on negative supercoiling, a process that keeps balance in bacterial DNA replication and prevents positive supercoiling from over twisting DNA and breaking DNA strands. Accordingly, DNA gyrase has a bright future for the survival of bacteria. The numerous amounts of DNA gyrase in prokaryotes like bacteria and their absence in human cells make them a selective target for newly developed molecules preserving both antibacterial and anti-MDR efficacy [43]. On the other hand, different mutations in gyrase lead to bacterial resistance, which results in their traditional drug candidates not working properly. Based on these aspects, DNA gyrase inhibitors are driving the interest of researchers towards designing and synthesizing further potent candidates with higher DNA gyrase inhibitory activity and improving their toxicity profiles.

1.1. Design rationale

In order to produce molecules with increased bioactivity, a key tactic in drug discovery is molecular hybridization, which combines several bioactive pharmacophores into a single molecular entity. Furthermore, researchers have acknowledged the significant role of nitrogen-containing heterocycles as structural motifs in the development of novel medications, particularly in the field of antimicrobial agents [44, 45]. Nitrogen and oxygen atoms produce a significant biological activity in heterocyclic structures by allowing them to interact with biological macromolecules like enzymes, proteins, and DNA [46–48].

Accordingly, herein molecular hybridization process was used to design and synthesize new hybrid molecules composed of benzofuran-pyrazole scaffold clubbed with various heterocycles, including pyridine, pyran, chromene, pyrano-pyrazole, pyrido-triazine, and triazolo-pyridine nuclei **(Figure 2)**.

In total, a series of new hybrid compounds have been created, and their molecular structures have been fully characterized. The antimicrobial characteristics of these compounds were examined against various fungal isolates, Gram-positive and Gram-negative bacteria. We also evaluated the new hybrids as in vitro antioxidants and anti-inflammatory agents. We selected the most promising compounds **9** and **10** as representative examples to study their suppression effects against the E. coli DNA gyrase B enzyme. Molecular docking and ADMET studies were also performed for the most active compound **9,** using *E. coli* DNA gyrase B as the target enzyme.

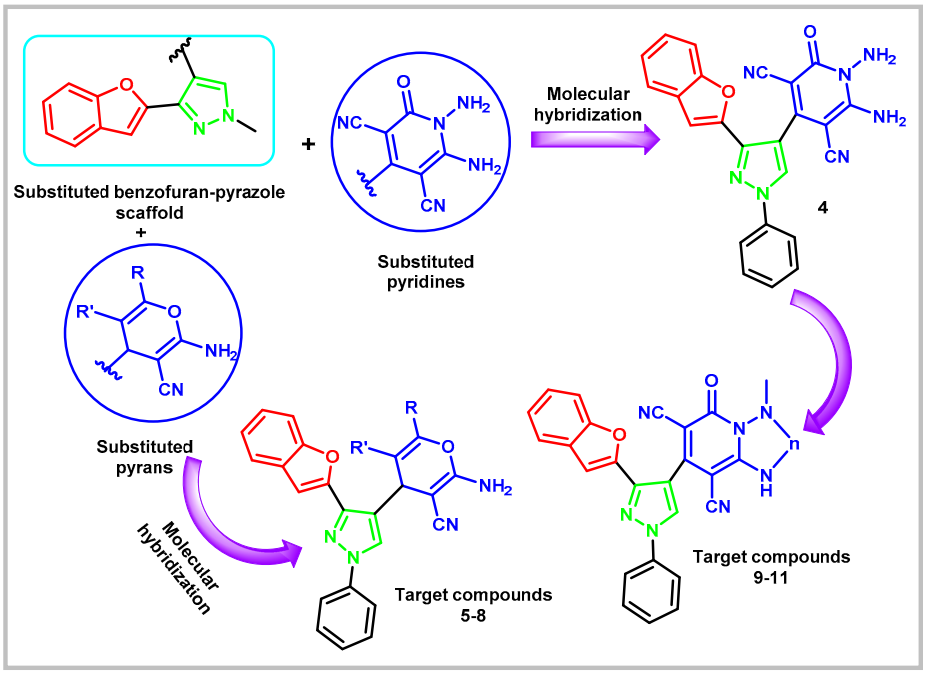

Figure 2. Development of new benzofuran-pyrazole hybrids of potential antimicrobial activity.

 doi:10.20944/preprints202408.1792.v2

2. Results and Discussion

2.1. Chemistry

Schemes 1-3 depict the synthetic pathways adopted for the preparation of the new benzofuranpyrazole hybrid derivatives in this study. Using the Vilsmeier-Haach reaction, the key starting material 3-(benzofuran-2-yl)-1-phenyl-1H-pyrazole-4-carbaldehyde **(1)** was prepared according to the reported method [17]. Compound **1** was condensed with malonitrile to form 2-((3-(benzofuran-2-yl)-1-phenyl-1H-pyrazol-4-yl)methylene) malonitrile **(2)** [17]. The compound 1,6-diamino-4-(3-(benzofuran-2-yl)-1-phenyl-1H-pyrazol-4-yl)-1,2-dihydro-2-oxopyridine-3,5-dicarbonitrile **(4)** was prepared in either two ways. Firstly, by refluxing the arylidine analogue **2** with cyanoacetohydrazide in absolute ethanol containing a catalytic amount of piperidine. Secondly, by condensation of the key starting aldehyde **1** with cyanoacetohydrazide to afford the cyanoacetohydrazide derivative **3,** which was further cyclized with malononitrile in absolute ethanol containing a few drops of piperidine to produce the desired compound **4**. The elemental analyses and spectral data confirmed the molecular structures of the synthesized derivatives. The IR spectrum of compound **3** showed characteristic absorption bands at 3261, 2266, and 1678 cm^{-1} that are attributed to NH, CN, and C=O groups, respectively. Its 1H NMR spectrum also showed four singlet signals at δ_H 3.86, 4.23, 8.50, 8.58, 9..04, 9.05, and 11.86 ppm. These were for the methylene group, the azomethine CH=N (E and Z isomers), pyrazole-H5, and NH protons, in that order. There were also multiplet signals for aromatic protons at μ 7.34–8.02 ppm. Also, the IR spectrum of compound **4** displayed strong absorption bands at 3300, 3241, 3196, 3131 ($2NH_2$), 2218 (2CN), and 1664 cm^{-1} (lactamic C=O). ^{1}H NMR spectrum of the same compound showed two D_2O exchangeable singlet signals at δ 5.72 and 8.58 ppm due to -C-NH_2 and -N-NH_2 protons, respectively. This result confirms the difference in the nucleophilicity between the two amino groups. Thus, it is expected that the hydrazide β-nitrogen (-N-NH_2) is more nucleophilic and will react more rapidly with the electron deficient carbon than the second amino group (-C-NH_2). The aromatic protons appeared as a multiplet signal in the range δ 7.17-8.01 ppm, while the pyrazole-H5 appeared as a singlet at δ 9.11 ppm. The mass spectrum further confirmed Compound 4, agreeing well with the assigned structure and displaying the correct molecular ion peak at m/z 433 **(Scheme 1)**.

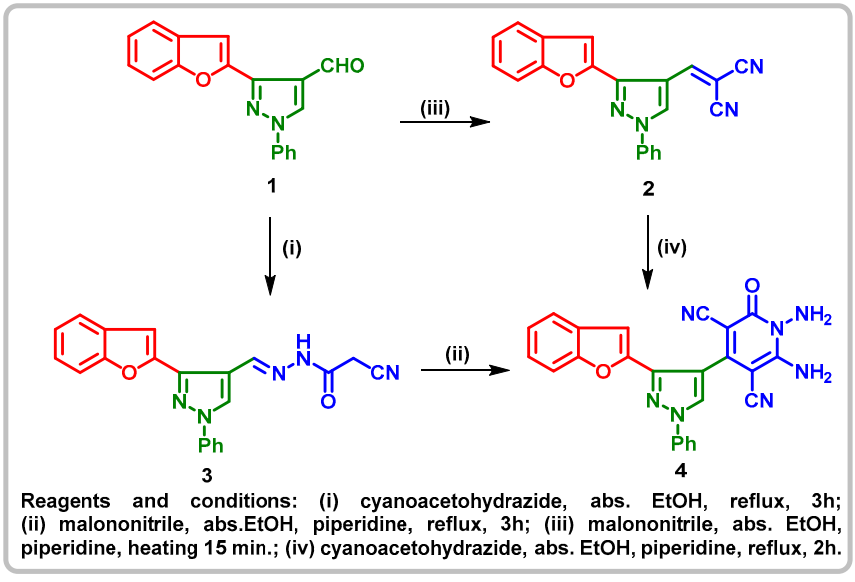

Scheme 1. Synthesis of 1,6-diamino-2-oxopyridine-pyrazolobenzofuran derivative **4.**

Moreover, condensation of the malononitrile derivative **2** with ethyl acetoacetate in the presence of a few drops of piperidine as a catalyst yielded the corresponding ethyl 6-amino-5-cyano-2-methyl-4*H*-pyran-3-carboxylate **5**. Furthermore, the treatment of the arylidine malononitrile derivative **2** with resorcinol and/or dimedone in absolute ethanol containing a catalytic amount of piperidine yielded the chromene derivatives **6**, **7**. Moreover, in order to obtain the fused pyrano[2,3-*c*]pyrazole

 doi:10.20944/preprints202408.1792.v2

compound **8**, the key intermediate **2** was treated with 3-methyl-1*H*-pyrazol-5(4*H*)-one derivative in absolute ethanol containing few drops of piperidine (**Scheme 2**).

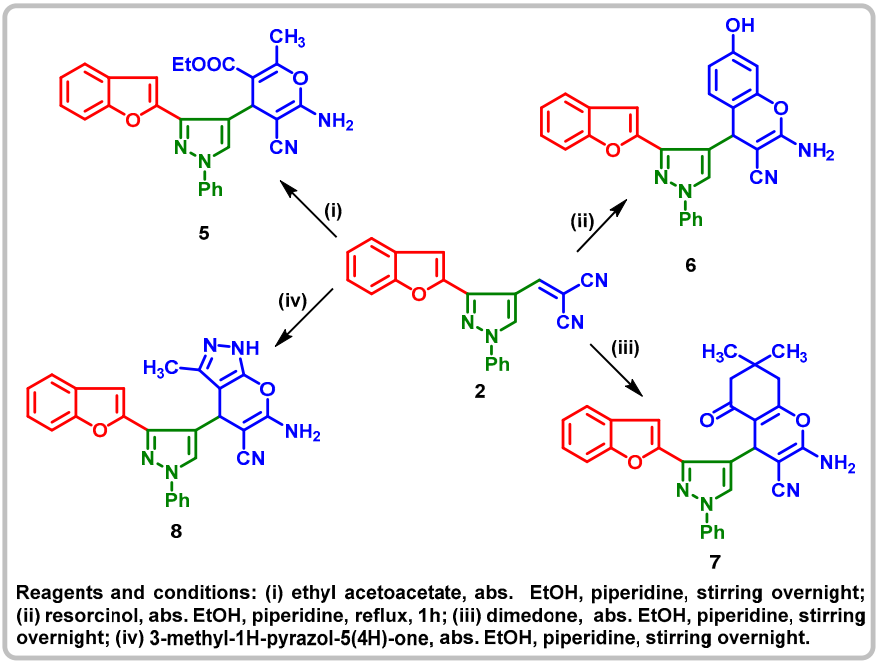

Scheme 2. Synthesis of pyrano, chromene, tetrahydrochromene, pyrano[2,3-*c*]pyrazole derivatives.

The structure of the new pyran derivative **5** was elucidated on the basis of elemental and spectral data. For example, ^{1}H NMR spectrum of compound **5** showed the characteristic triplet-quartet signals of the carboxylate group at δ 0.90 and 3.91 ppm, respectively. Additionally, the ^{1}H NMR spectrum of compound **5** revealed four singlets at approximately δ 2.28, 4.45, 5.04, and 7.71 ppm, which correspond to the protons of CH_3, NH_2, pyran-H4, and pyrazole-H5, respectively, in addition to the multiplet signals of the aromatic protons, which appeared in the range of approximately δ 7.17–7.70 ppm. Its ^{13}C NMR spectrum displayed three signals at δ 13.87, 18.58, and 61.79 ppm related to the methyl and ethyl carbons, respectively, besides the other signals attributed to the expected carbons of the molecule. The chemical structures of the obtained chromene and tetrahydrochromene derivatives **6**, **7** were confirmed by elemental and spectral analyses. For example, the IR spectrum of compound **6** represented absorption bands at 3325, 3204, 3135, and 2197 cm^{-1} that contributed to OH, NH_2, and CN groups, respectively. The ^{1}H NMR spectrum of the same analogue displayed three singlets at δ 5.21, 7.19, and 8.61 ppm attributed to the pyran-H4, OH, and pyrazole-H5, respectively. While ^{1}H NMR spectrum of compound **7** exhibited two singlet signals at δ 0.64 and 0.93 ppm referring to two methyl groups, there were also three singlet signals at 4.69, 6.99, and 8.53 ppm, indicating the protons chromene-H4, NH_2 group, and pyrazole-H5, respectively. In addition, the ^{13}C NMR spectrum of **7** represented, besides the expected cyano and aromatic signals, characteristic signals at δ 26.59, 26.97, 28.86, 32.00, 50.52, 57.96, and 196.34 ppm due to the carbons of 2-CH_3, CH_2, chromene-C7, chromene-C6, chromene-C3, and C=O, respectively. The elemental and spectral data confirmed the chemical structure of compound **8**. The IR spectrum of the latter compound **8** showed characteristic absorption bands in the range 3393-3176 cm^{-1} due to NH and NH_2, and at 2186 cm^{-1} due to the CN group. The ^{1}H NMR spectrum exhibited a singlet signal at δ 1.83 ppm attributed to CH_3, besides the other signals that appeared in their expected regions. The ^{13}C NMR spectrum represented a signal at δ 10.25 ppm assignable to the CH_3 group, in addition to other 24 signals representing the cyano and aromatic carbons of the molecule (**Scheme 2**).

O-Diamines are ready-made nucleophilic centres for the synthesis of fused nitrogen heterocyclic rings. Thus, diaminopyridone **4** was a useful building block for the synthesis of nitrogen bridge-head pyrido-triazine and/or pyrido-triazole derivatives **9**, **10**, **11a-d**, respectively. Upon the treatment of diaminopyridone **4** with 1,2-dibromoethane in pyridine produced the corresponding tetrahydro-1H-

 doi:10.20944/preprints202408.1792.v2

pyrido[1,2-b][1,2,4]triazine derivative **9**. Furthermore, the 1,2,4-triazolo[1,5-a]pyridine and tetrahydro-[1,2,4]-triazolo[1,5-a]pyridine derivatives **10, 11a-d** were obtained by boiling of the diaminopyridone derivative **4** in acetic anhydride and/or its refluxing with different aldehydes in acetic acid, respectively (**Scheme 3**).

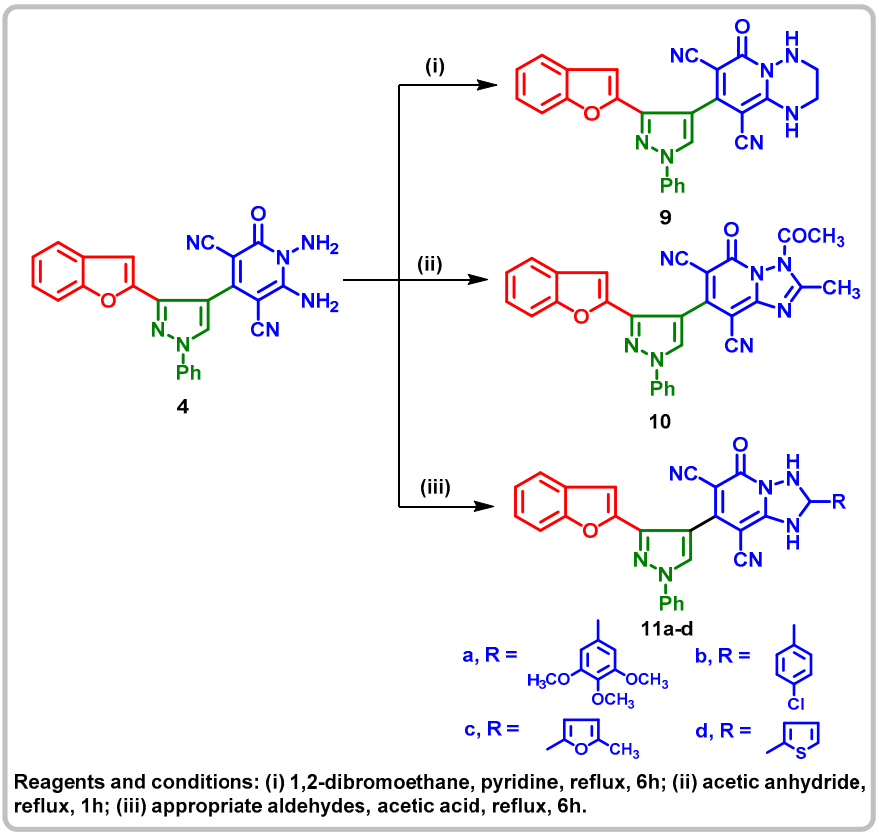

Scheme 3. Synthesis of pyrido[1,2-*b*][1,2,4]triazine and [1,2,4]triazolo[1,5-*a*]pyridine derivatives.

Elemental analysis and spectral data (IR, MS, ^{1}H and ^{13}C NMR spectra) confirmed the reaction product. IR spectrum of compound **9** showed absorption bands at 3189, 3127, and 2213 cm^{-1} due to 2NH and 2CN groups, respectively. In addition, its ^{1}H NMR spectrum displayed the methylene protons of 2CH$_2$ as two multiplets at δ 2.07, 2.43 ppm, in addition to the aromatic protons, pyrazole-H5, and 2NH protons that appeared at their expected regions. Furthermore, the ^{13}C NMR spectrum of the compound **9** exhibited 25 carbon signals, the most important signals appeared at δ 31.12, 71.45, and 161.64 ppm characteristic for the two methylene and carbonyl carbons, respectively. IR spectrum of compound **10** showed the disappearance of NH$_2$ bands of the parent diaminopyridone **4** and the presence of two absorption bands at 2223, 1671 cm^{-1} referring to 2CN and 2CO groups, respectively. Also, ^{1}H NMR spectrum of compound **10** revealed, in addition to the aromatic protons and pyrazole-H5, two characteristic singlet signals at δ 1.92, 2.09 ppm attributed to the methyl and acetyl protons, respectively. While its ^{13}C NMR spectrum displayed 24 carbon signals, representing the methyl and acetyl carbons at δ 21.56 and 31.19 ppm, respectively. At the same time, the elemental analyses and spectral data were consistent with the proposed tetrahydro-[1,2,4]-triazolo[1,5-a]pyridine derivatives **11a-d**. For example, ^{1}H NMR spectrum of compound **11a** revealed two singlets at δ 3.79, 3.89 ppm assignable to 3 (OCH$_3$) and three other singlet signals at δ 8.56, 8.90, and 9.13 ppm attributable to the respective protons of 2NH, triazole-H3, and pyrazole-H5, respectively. Furthermore, the ^{1}H NMR spectrum of **11c** exhibited, besides the expected signals of the aromatic protons, four singlets at δ 2.40, 8.70, 9.07, and 9.12 ppm due to the protons of CH$_3$, 2NH, and pyrazole-H5, respectively. In addition, the furan-H3, H4 appeared as two douplets at δ 6.51, 6.96 ppm, respectively. Mass spectra of **11a-d** showed the molecular ion peaks, which were in agreement with their molecular formulae (**Scheme 3**).

 doi:10.20944/preprints202408.1792.v2

2.2. Biological Evaluation

2.2.1. Antimicrobial Activity Determination

The *in vitro* antimicrobial activity of the new target compounds was evaluated against two fungal isolates, *F. solani* and *C. albicans* ATCC-10231; four bacterial isolates, *S. aureus* ATCC 6538 and *B. cereus* ATCC 11778, as Gram-positive bacteria; and *E. coli* 25922 and *P. aeruginosa* ATCC 27853 as Gram-negative bacteria. These specific strains were chosen because of their ability to form biofilms and their major impact on human health. Using the agar-well diffusion method [49], the average diameter of the inhibition zones in millimetres was assessed for each tested compound (10 µg/mL) against each type of microbial growth surrounding the discs **(Table 1)**.

Table 1. The antimicrobial potency of the new target benzofuran-pyrazole based derivatives, expressed as inhibition zone (mm).

Mean diameter of zones of inhibition (Mean ± SEM) (mm)						
Compd. No.	**Gram +ve Bacteria**		**Gram -ve Bacteria**		**Fungi**	
	S. aureus ATCC 6538	***B. cereus ATCC-11778***	***E. coli ATCC-25922***	***P. aeruginosa ATCC-27853***	***F. solani***	***C. albicans ATCC-10231***
2	15	13	18	20	12	12
3	15	14	15	18	12	13
4	15	15	15	17	17	15
5	15	12	14	20	12	11
6	14	12	15	17	0	0
7	15	14	15	15	17	16
8	20	16	15	17	16	15
9	**20**	**18**	**15**	**20**	**16**	**20**
10	**22**	**19**	**15**	**20**	**20**	**20**
11a	15	12	15	18	15	0
11b	**20**	15	15	20	15	16
11c	20	15	17	20	12	15
11d	**20**	15	16	17	15	19
N*	20	20	25	24	-	-
C*	-	-	-		20	14

Antibacterial Standard; N*= Novobiocin (30 µg), antifungal Standard; C*= Clotrimazole (50 µg).

Also, the double-sequence dilution method [50–52] was used to find the minimum inhibitory concentration (MIC) values (given in µM) for the promising compounds with an IZ of 15 mm or more (**4**, **7**, **8**, **9**, **10**, **11b–d**) against all the tested isolates. Novobiocin (30 µg) and clotrimazole (50 µg) were utilized as the standard antibiotic and antifungal drugs, respectively, and the results were recorded in **Table 2**.

Table 2. MIC values of the most active analogues against various microbial species **(µM).**

Compd. No.	**Gram +ve Bacteria**		**Gram -ve bacteria**		**Fungi**	
	S. aureus ATCC 6538	***B. cereus ATCC-11778***	***E. coli ATCC-25922***	***P. aeruginosa ATCC-27853***	***F. solani***	***C. albicans ATCC-10231***
4	15	15	15	17	27	25
7	15	14	15	15	**27**	**30**
8	20	16	15	17	35	25
9	**2.50**	**4.65**	**5.79**	**17.60**	**20**	**16**
10	**3.49**	**8.80**	**4.65**	**20**	**16**	**14**
11b	**5.11**	**8.60**	**8.69**	**17.0**	**15**	**16**

 doi:10.20944/preprints202408.1792.v2

11c	**5.90**	**7.79**	**16.0**	**16.90**	**15**	**19**
11d	**5.11**	**15**	**16.0**	**20**	**15**	**19**
N*	3.49	6.98	4.65	18.6	-	-
C*	-	-	-	-	20	14

Antibacterial Standard; N*= Novobiocin (30 µg), antifungal Standard; C*= Clotrimazole (50 µg).

Based on MIC results, it was noticed that all of the tested strains were susceptible to the antibacterial characteristics of the examined compounds. It was detected that the nitrogen bridge-head pyrido-triazine and/or pyrido-triazole derivatives **9**, **10**, and **11b-d**, respectively, were the most promising candidates as broad-spectrum antimicrobial members. While it showed an equivalent activity to clotrimazole against the examined fungal strains (MIC = 20, 16 µg/mL, $MIC_{Clotrimazole}$= 20, 14 µg/mL), the six-membered pyrido-triazine compound **9** produced more significant potency than novobiocin against the tested positive and negative bacterial isolates (MIC= 2.50 -17.60 µg/mL, $MIC_{novobiocin}$= 3.49-18.6 µg/mL). On the other hand, the 2-methyl-triazolo[1,5-*a*]pyridine derivative **10** has emerged as a potent antifungal candidate. It showed more significant activity against the fungal strain *F. solani* than clotrimazole, with an MIC value of 16µg/mL, and equivalent antifungal activity to the reference drug against the tested *C. albicans* isolates, with an MIC value of 14µg/mL. The antibacterial efficacy of the latter derivative appears to be slightly lower than that of the reference novobiocin, with MIC values ranging from 3.49 to 20 µg/mL.

Interestingly, changing the 2-methyl group in compound **10** to different phenyl groups in compounds **11b,c** increased their antifungal activity more than clotrimazole, with MIC values ranging from 16–19 µg/mL. However, they decreased their antibacterial activity against the tested bacterial isolates, with MIC values ranging from 5.11–20 µg/mL, which was lower than novobiocin. Conversely, the rest of the target compounds **4**, **7**, and **8** exhibited moderate antimicrobial activity with MIC values ranging from 14 to 30 µM. Taken together, it could be concluded that the pyrido-triazine and/or pyrido-triazole ring system attached to the pyrazol-benzofuran scaffold is a highly recommended feature for gaining significant broad spectrum antimicrobial efficacy.

2.2.2. Antioxidant Activity

Free radicals display an integral role in normal physiological functions such as cell signaling, immunological response, and overall redox homeostasis maintenance [53]. Reactive oxygen and nitrogen species (ROS/RNS) are naturally produced through the cellular metabolism. They act as "redox messengers" in signaling pathways and are helpful against infectious pathogens, but they can also cause detrimental oxidative stress [53]. The relationship between endogenous and exogenous antioxidant systems regulates the level of radical activity. Excess radicals can cause severe oxidation and damage to a variety of biomolecules, which can result in dysfunction or even cell death. Numerous neurological diseases, cancer, diabetes, high blood pressure issues, infectious diseases, and cardiovascular diseases, are believed to be associated with free radical damage [54, 55]. Antioxidants are compounds that reduce free radical concentrations and thus act as a protective barrier against the damage they cause to the body, which is why they are crucial in the prevention of various diseases.

Many processes have been described to evaluate the antioxidant activity of specific compounds, but the most widely documented relates to the 2,2-diphenyl-1-picrylhydrazyl (DPPH) radical [56] using the DPPH-free radical scavenging assay utilizing ascorbic acid as a standard drug, and results were presented in **Table 3.** The obtained antioxidant activity of the tested compounds varied from moderate to potent activity in comparison with ascorbic acid. The most potent scavenging activity was produced by the compounds **4**, **6**, **9**, **11b, and 11d** (%DPPH scavenging activity = 84.16, 86.42, 85.87, 90.52, 88.56, and 89.42%, respectively). On the other hand, the rest of the derivatives appeared to be moderate-to-weak antioxidant candidates **(Figure 3)**. Fortunately, the most potent antimicrobial pyrido-triazine derivative **9** produced an effective radical scavenging capacity (88.56±0.43%).

2.2.3. Anti-Inflammatory Assay

 doi:10.20944/preprints202408.1792.v2

The new target compounds were assessed for their *in vitro* anti-inflammatory potential via the HRBC membrane stabilization process. The anti-inflammatory effectiveness of the compounds was determined by regulating the suppression of hypotonicity-induced HRBC membrane lysis, which is an inflammatory response.

The HRBC membrane can be viewed as a model of the lysosomal membrane, which is crucial in inflammation. Stabilization of the lysosomal membrane plays a key role in controlling inflammatory reactions [57]. The mechanism involves the release of lysosomal contents of active neutrophils, such as bactericidal enzymes and proteases, which, upon extracellular release, produce further tissue inflammation and injury, which is said to be acute or chronic inflammation [57].

The HRBC membrane stability test relies on the discovery that non-steroidal anti-inflammatory drugs prevent erythrocyte lysis, most likely by maintaining the cell membrane's stability. Inflammatory symptoms may be alleviated by compounds that stop the lysis of the HRBC membrane brought on by the release of hydrolytic enzymes from lysosomes [58].

The mechanism of action for compounds' membrane protection may involve their binding to HRBC membranes and altering the charges on the cell surface [59, 60]. Alternatively, it may involve the deformation of cells through interactions with other compounds or membrane proteins in the erythrocyte membranes. Later on, this contact can cause changes to the cell surface charges or their ability to adjust the intracellular concentration of calcium into the erythrocytes [61]. Accordingly, it was of interest to predict the anti-inflammatory activity *in vitro* of the new analogues according to the reported method [62].

The percentage of HRBC membrane stabilization tests for the newly synthesized derivatives and the positive control aspirin and diclofenac sodium were carried out, and the results are provided in **Table 3**.

Most of the examined derivatives showed significant HRBC membrane stabilization and protection percentages ranging from 86.70±0.259 to 99.25±0.108%. Unfortunately, less protection% and weak activity were determined by compounds **11c** and **10** (73.67±0.388 and 29.67±0.496%, respectively). Interestingly, the most active antimicrobial analogue **9** showed promising protection% (86.70±0.259%) **(Figure 4).**

Table 3. *In vitro* anti-inflammatory and antioxidant activities of the new target benzofuran-pyrazole based derivatives.

Compound No.	Anti-inflammatory		Antioxidant activity
	% Hemolysis	% Protection	%DPPH radical scavenging activity
2	0.82±0.108	99.25±0.108	71.19±0.43
4	0.67±0.194	99.19±0.194	84.16±4.41
5	0.76±0.151	99.13±0.151	58.10±0.52
6	0.76±0.086	99.18±0.086	86.42±2.85
7	2.38±0.173	97.50±0.173	37.06±1.38
8	1.43±0.173	98.44±0.173	7.89±1.04
9	**13.12±0.259**	**86.70±0.259**	**88.56±0.43**
10	70.68±0.496	29.67±0.496	48.93±0.09
11a	1.37±.086	98.57±0.086	47.16±3.03
11b	6.16±0.755	93.30±0.755	89.42±1.56
11c	26.60±0.388	73.67±0.388	60.61±2.34
11d	2.84±0.259	97.35±0.259	77.00±0.26
Aspirin	1.98±0.173	97.90±0.173	**----**
Diclofenac	0.46±0.043	99.51±0.043	-----
Ascorbic acid	----	----	100±0.00

 doi:10.20944/preprints202408.1792.v2

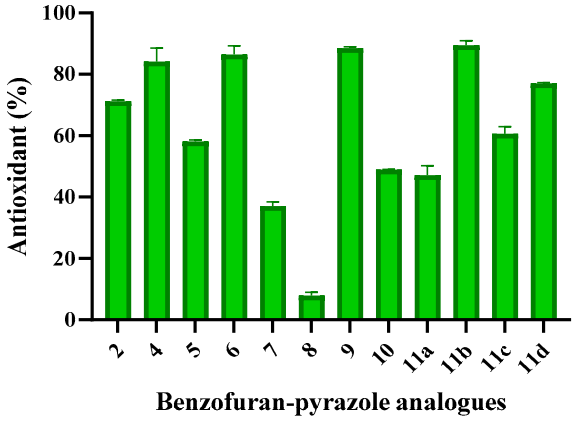

Figure 3. Antioxidant activities of the new target benzofuran-pyrazole based derivatives.

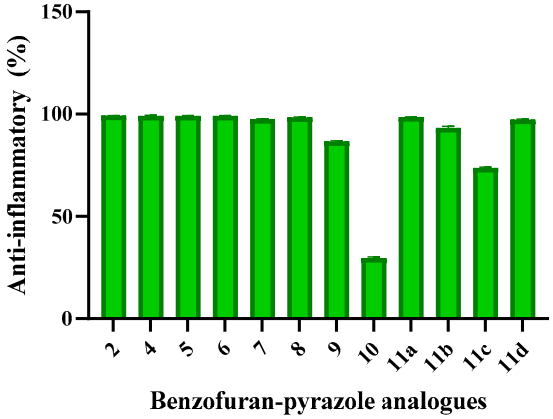

Figure 4. Anti-inflammatory activity of the new target benzofuran-pyrazole-based derivatives.

2.2.4. E. coli DNA Gyrase B Suppression Effect

The compounds that exhibited the most promising antimicrobial, antioxidant, and anti-inflammatory activities, **9** and **10**, were evaluated for *in vitro* suppression effects against *E. coli* DNA gyrase B as a trial to find out their modes of action as antimicrobial candidates [62–64], where ciprofloxacin was served as a standard drug **(Table 4)**.

The results demonstrated that the pyrido-triazine compound **9** produced a more potent suppression impact against *E. coli* DNA gyrase B than **10**, but it was slightly less potent than ciprofloxacin, with IC_{50}s of 9.80±0.21, 32.20 ± 0.10, and 8.03 ±0.03, respectively. The increase in the ring size attached to the benzofuran-pyrazole mother scaffold led to a greater suppression effect, which could be explained by the creation of an additional hydrophobic interaction with *E. coli* DNA gyrase B, resulting in an increase in the fitting of the compound in the active sites of the tested enzyme.

2.2.5. In Vitro Cytotoxicity Assay

In continuation of this study, the safety profiles of the analogues **9**, and **10** were assessed utilizing the calorimetric cell proliferation MTT [64] to evaluate the cytotoxic effects against the human diploid cell line WI-38, which is derived from lung tissues. **Table 4** shows that the compounds' safety profiles looked good and were much better than those of the standard drug ciprofloxaxin (IC_{50}s = 163.3± 0.17, 170 ± 0.40, and 86.2± 0.03 μM, respectively).

Table 4. Assessment of inhibitory potential of compounds **9**, **10** against *E. coli* DNA gyrase B in relation to Novobiocin.

 doi:10.20944/preprints202408.1792.v2

Compound No.	IC_{50} (mean±SEM) (μM)	
	E. coli DNA gyrase B	Cytotoxicity WI38
9	9.80±0.21	163.3± 0.17
10	32.20 ± 0.10	170 ± 0.40
Ciproloxacin	8.03 ±0.03	86.2± 0.03

2.3. In Silico Studies

2.3.1. Molecular Docking

Despite docking software's capacity to identify potential binding modes between a ligand and its target, it is still an unreliable method that requires constant verification. As a result, the docking procedure was initially verified by re-docking the co-crystallized ligand close to the enzyme's binding site. For the co-crystallized ligand of the DNA gyrase enzyme, the root mean square deviation (RMSD) was found to be 0.23 indicating a successful docking technique (**Figure 5**).

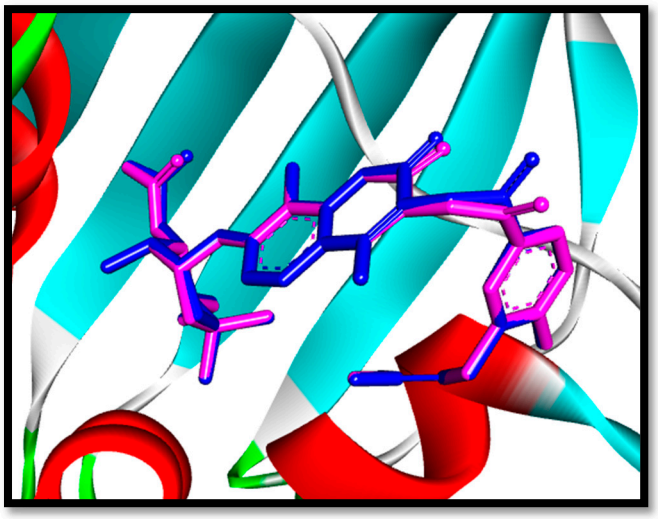

Figure 5. 3D representation of the superimposition of the co-crystallized (purple) and the docking pose (blue) of novobiocin in the active site of *E. coli* DNA gyrase.

Compound **9** has the ability to bind to DNA gyrase active site in a comparable pattern to the co-crystallized ligand; novobiocin. It shows a binding energy score of -8.9 kcal/mol. compared to -9.4 kcal/mol. for novobiocin. Compound **9** binds the key amino acids Arg1027, Asp81, Pro1075 and Glu1046 through pi-anion and pi-cation interactions in addition to supportive hydrophobic interactions with different amino acid residues in the vicinity of the active site **(Figure 6)**.

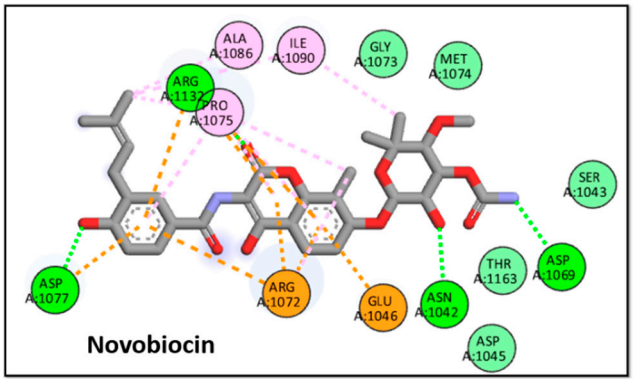

 doi:10.20944/preprints202408.1792.v2

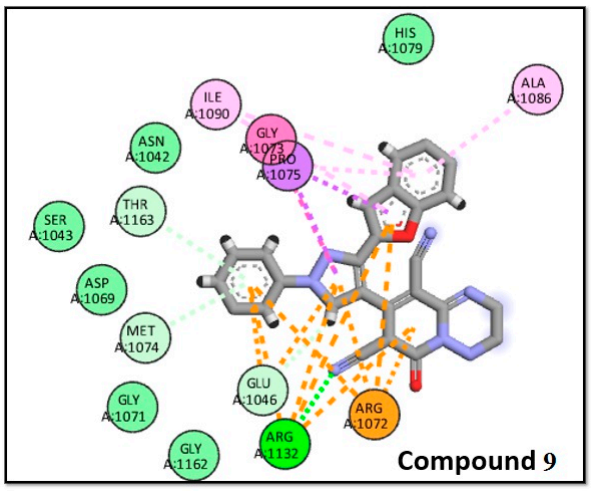

Figure 6. The binding interactions of novobiocin against the tested compound **9** against *E. coli* DNA gyrase active site (pdb: 4URO).

The binding energy scores of all the synthesized derivatives are summarized in **Table 5.**

Table 5. Binding energy scores of the synthesized compounds (kcal./mol).

Compound No.	Energy Score (kcal/mol.)	Compound No.	Energy Score (kcal/mol.)
4	-8.2	**10**	-8.7
5	-8.4	**11a**	-8.4
6	-8.6	**11b**	-8.1
7	-8.1	**11c**	-7.9
8	-8.3	**11d**	-8.2
9	-8.9	**Novobiocin**	-9.4

2.3.2. ADMET Studies

Several measures are calculated by the SwissADME webserver to predict its oral bioavailability, pharmacokinetic properties, BBB penetration possibility, and permeability glycoprotein (PGP) binding affinity. The bioavailability radar chart of the tested derivatives is illustrated in **Figure 7**. Compound **9** shows only one violation out of six measured parameters: lipophilicity (LIPO), size, polarity, insolubility (INSOL), insaturation (INSATU), and flexibility (FLEX); the violation was in the insaturation parameter (**Figure 8**). A BOILED-EGG chart was constructed; the white area indicates gastro-intestinal absorption, while the non-mutually exclusive yellow area indicates BBB penetration. The blue color indicates the high possibility of the tested compound being a substrate for PGP, which is an efflux protein responsible for uptake and efflux of many drugs; a red color means the lower possibility of being a PGP substrate [67].

Among all the tested compounds, compound **9** shows the highest gastro-intestinalabsorption with no BBB penetration, but it's a possible substrate for PGP (**Figure 8**). Eventually, applying Lipinski's rule of five [68] which is a four-rule fulfilment criteria that is calculated to predict the drug-likeness of the tested derivative, 11 has a predicted logP value of 2.67 (<5), a molecular weight of 459.46 g/mol (<500), 9 hydrogen bond acceptor groups (7 nitrogens + 2 oxygens) (<10), and only 2 hydrogen bond donor groups (2 NH) (<5), and so shows no violation of Lipinski's rule, indicating its good pharmacokinetic profile.

Table 7. Prediction of physicochemical and AMDE properties of 4-11 employing SwissADME.

Co	mp	ou	Mo	lec	ula	#	Rot	#	H-	#	H-	Mo	lar	TP	SA	Lo	g *P*	GI	abs	orp	BB	B	P-	gp	Lip	ins	ki	Bio	ava	ila	Sy	nth	etic
	4		433.42			3		5		2		122.44		152.58 Å²		2.33		Low		No			Yes		0		0.55			3.7			

 doi:10.20944/preprints202408.1792.v2

5	466.49	6	6	1	128.77	116.30 Å²	3.78	Low	No	No	0	0.56	4.61
6	446.46	3	5	2	126.22	110.23 Å²	3.92	High	No	Yes	0	0.55	4.44
7	476.53	3	5	1	134.92	107.07 Å²	4.24	Low	No	No	0	0.56	4.78
8	434.45	3	5	2	121.31	118.68 Å²	3.44	High	No	Yes	0	0.55	4.44
9	459.46	3	5	2	136	124.60 Å²	2.67	High	No	Yes	0	0.55	3.96
10	499.48	4	7	0	138.1	134.91 Å²	3.14	Low	No	Yes	0	0.55	3.92
11a	611.61	7	8	2	175.16	152.29 Å²	3.69	Low	No	Yes	2	0.17	5.12
11b	555.97	4	5	2	160.69	124.60 Å²	4.27	Low	No	No	1	0.55	4.66
11c	525.52	4	6	2	152.92	137.74 Å²	3.51	Low	No	Yes	1	0.55	4.72
11d	527.56	4	5	2	153.56	152.84 Å²	3.81	Low	No	Yes	1	0.55	4.60

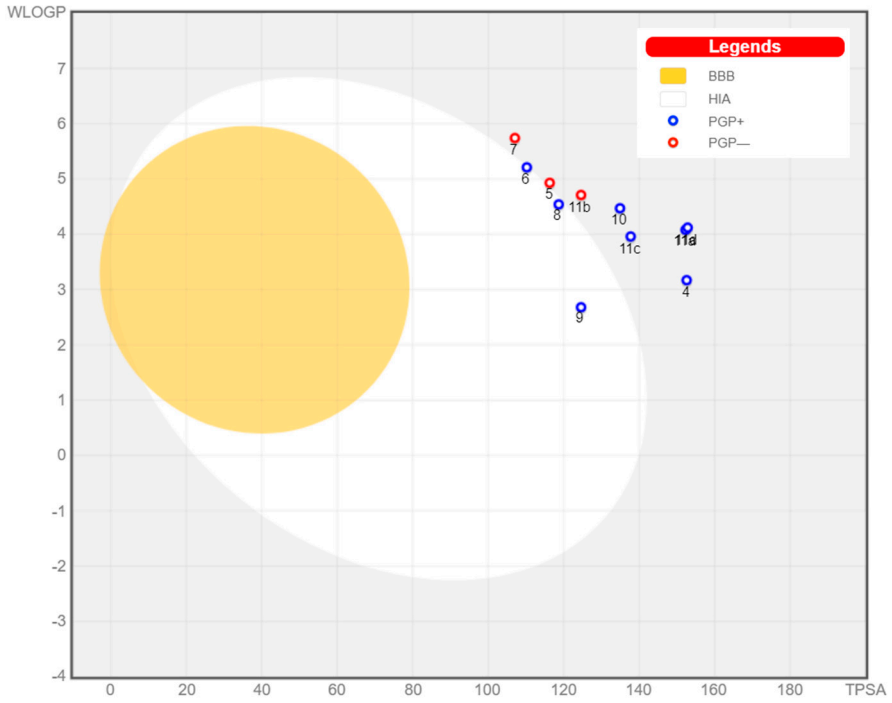

Figure 8. BOILED-EGG chart for compounds 4-11d (the blue circle represents the tested compound).

3. Conclusions

Based on the molecular hybridization process, new hybrid molecules composed of benzofuran-pyrazole scaffolds are conjugated with different *N*/*O* heterocyclic rings, such as pyridine, pyran, chromene, pyrano-pyrazole, pyrido-triazine, and triazolo-pyridine cores. The newly synthesized target compounds were characterized using microanalysis and spectroscopic approaches. In addition, the new analogues were evaluated as antimicrobial candidates against various strains of both Gram-positive and Gram-negative bacteria as well as fungi in comparison with novobiocin and clotrimazole as antibacterial and antifungal standard drugs. Promising broad-spectrum antimicrobial potency against the examined bacterial and fungal species was observed by the pyrido-triazine and/or pyrido-triazole derivatives 9, 10, and 11b-d, respectively, with MIC values ranging from 2.50–20 µg/mL. All the new hybrids were also examined as *in vitro* antioxidants and anti-inflammatory agents using DPPH-free radical scavenging assays and HRBC membrane stabilization processes, respectively. Compounds 4, 6, 9, 11b, and 11d exhibited the most potent scavenging activity (%DPPH scavenging activity = 84.16 - 90.52%), while all of the examined compounds (except 11c and 10) showed significant HRBC membrane stabilization and protection percentages ranging from 86.70±0.259 to 99.25±0.108%. Moreover, the most promising antimicrobial, antioxidant, and anti-inflammatory activities, 9 and 10, were evaluated for *in vitro* suppression effects against *E. coli* DNA gyrase B to find out their expected modes of action as antimicrobial candidates. The compound 9 was a more potent inhibitor against DNA gyrase B than 10, with IC_{50}s of 10.71 and 19.58, respectively.

 doi:10.20944/preprints202408.1792.v2

Both 9 and 10 revealed promising safety profiles against the normal human diploid cell line WI-38 cell line, which were significantly superior to that obtained by the reference drug novobiocin (IC_{50}s = 140 ± 0.36, 165 ± 0.40, 163.3 ± 0.17, and 86.2 ± 0.09 µM, respectively).

The hero candidate in this study was the pyrido-triazine derivative 9, which demonstrated significant broad-spectrum antimicrobial activity with a radical scavenging capacity of 88.56±0.43%, a haemolytic protection rate of 86.70±0.259%, and *an E. coli* DNA gyrase B suppression impact with a promising safety profile. As a result, it could be considered a basic scaffold for the further development of new antimicrobial agents that help overcome the drug resistance phenomenon.

4. Experimental protocols

4.1. Chemistry

All melting points are uncorrected and were taken in open capillary tubes using Electrothermal apparatus 9100. The instruments used to determine melting points, spectral data (IR, ^{1}H NMR, ^{13}C NMR, and Mass), as well as chemical analyses were included in a detailed description in the file of Supporting Information. 3-(Benzofuran-2-yl)-1-phenyl-1*H*-pyrazole-4-carbaldehyde **(1)** and 2-((3-(benzofuran-2-yl)-1-phenyl-1*H*-pyrazol-4-yl)methylene)malononitrile **(2)** were prepared according the reported method [17].

4.1.1. N'-((3-(benzofuran-2-yl)-1-phenyl-1H-pyrazol-4-yl)methylene)-2-cyanoacetohy drazide (3)

A mixture of 3-(benzofuran-2-yl)-1-phenyl-1*H*-pyrazole-4-carbaldehyde (**1**) (2.88 g, 0.01 mol) and cyanoacetohydrazide (0.99 g, 0.01 mol) in absolute ethanol (30 mL) was refluxed for 3 h. Upon cooling, the formed precipitate was filtered, dried, and recrystallized from ethanol to give the title compound **3**.

Yield 61%, mp. 211-213°C, yellow powder; IR (KBr, cm^{-1}): 3261 (NH), 3059 (CH-arom.), 2959, 2917 (CH-aliph.), 2267 (CN), 1678 (C=O, amide); ^{1}H NMR (500 MHz; DMSO-d_6) δ_H 3.86 (s, 2H, CH_2, Z-isomer), 4.23 (s, 2H, CH_2, E-isomer), 7.34-7.43 (4H, m, Ar-H), 7.53-7.59 (2H, m, Ar-H), 7.64-7.74 (2H, m, Ar-H), 7.95-8.02 (2H, m, Ar-H), 8.50 (s,1H, CH=N, E-isomer), 8.58 (s,1H, CH=N, Z-isomer), 9.04 (s, 1H, pyrazole-H5, Z-isomer), 9.05 (s, 1H, pyrazole-H5, E-isomer), 11.86 (s, 1H, NH, D_2O exchangeable); ^{13}C NMR (125 MHz; DMSO-d_6) E-isomer δ_C 24.58 (CH_2), 105.68, 111.71, 116.65, 117.92, 119.38, 122.09, 123.99, 125.68, 127.92, 128.50, 129.43, 130.13, 137.88, 139.24, 140.94, 142.38, 14.53, 154.73 (aromatic-C), 160.94 (CO), ^{13}C NMR (125 MHz; DMSO-d_6) Z-isomer δ_C 25.34, 107.03, 111.71, 116.65, 117.92, 119.47, 122.09, 123.99, 125.68, 127.92, 128.69, 129.43, 130.16, 137.88, 139.24, 140.94, 142.47, 149.53, 154.73(aromatic-C), 159.33 (CO); MS, m/z (%): 369 $[M]^+$ (12), 285 $[C_{18}H_{11}N_3O]^+$ (8), 77 $[C_6H_5]^+$ (100); Anal. For $C_{21}H_{15}N_5O_2$ (369.38): Calcd. C, 68.28; H, 4.09; N, 18.96; Found: C, 68.34; H, 4.24; N, 18.71.

4.1.2.1,6-. Diamino-4-(3-(benzofuran-2-yl)-1-phenyl-1H-pyrazol-4-yl)-1,2-dihydro-2-oxopyridine-3,5-dicarbonitrile (4)

Method (A):

A mixture of 2-((3-(benzofuran-2-yl)-1-phenyl-1*H*-pyrazol-4-yl)methylene)malononitrile (**2**) (3.36 g, 0.01 mol) and cyanoacetohydrazide (0.99 g, 0.01 mol) in absolute ethanol (30 mL) containing 3-5 drops of piperidine was refluxed for 2h. The white precipitate obtained during heating was filtered, dried and recrystallized from ethanol to give the title compound **4**.

Method (B):

A mixture of compound **3** (1.85 g, 0.005 mol) and malononitrile (0.33 g, 0.005 mol) in absolute ethanol (20 mL) containing 3-5 drops of piperidine was refluxed for 3h. The white precipitate obtained during heating was filtered, dried and recrystallized from ethanol to give the title compound **4**.

Yield 85% (A), 80% (B); mp 269-270°C; IR (KBr, cm^{-1}): 3393, 3315, 3210 ($2NH_2$), 2217 (CN), 1661 (CO); ^{1}H NMR (300 MHz; DMSO-d_6) δ_H 5.72 (s, 2H, NH_2, D_2O exchangeable), 7.17 (s, 1H, Ar-H), 7.27-7.47 (m, 3H, Ar-H), 7.59-7.70 (m, 4H, Ar-H), 8.01 (d, 2H, ^3J = 7.8 Hz, Ar-H), 8.58 (br, 2H, NH_2, D_2O exchangeable), 9.11 (s, 1H, pyrazole proton) ppm; ^{13}C NMR (75 MHz; DMSO-d_6) δ_C 76.00, 88.18, 105.39, 111.81, 115.80, 115.86, 116.72, 119.18, 122.06, 123.91, 125.69, 128.04, 128.63, 130.40, 139.11,

 doi:10.20944/preprints202408.1792.v2

141.57, 148.52, 151.38, 154.61, 157.17, 159.74; MS, m/z (%): 433 $[M]^+$ (37), 434 $[M]^{+1}$ (19), 77 $[C_6H_5]^+$ (100). Anal. calcd. for $C_{24}H_{15}N_7O_2$ (433.43): C, 66.51; H, 3.49; N, 22.62; found: C, 66.32; H, 3.22; N, 22.43.

4.1.3. Ethyl-6-amino-4-(3-(benzofuran-2-yl)-1-phenyl-1H-pyrazol-4-yl)-5-cyano-2-methyl-4H-pyran-3-carboxylate (5)

A mixture of compound **2** (0.68 g, 0.002 mol) and ethyl acetoacetate (0.26 ml, 0.002 mol) in absolute ethanol (20 mL) containing 2-3 drops of piperidine was stirred overnight at room temperature. The formed precipitate was filtered, dried and recrystallized from ethanol to give the title compound **5**.

Yield 76%, mp. 196-198°C, white powder; IR (KBr, cm^{-1}): 3315, 3188, (NH_2), 3062 (CH-arom.), 2980, 2924 (CH-aliph.), 2201 (CN), 1725 (C=O, ester); ^{1}H NMR (300 MHz; $CDCl_3$) δ_H 0.90 (t, 3H, ^3J = 7.2 Hz, $CO_2CH_2CH_3$), 2.28 (s, 3H, CH_3), 3.91 (q, 2H, ^3J = 6.8 Hz, $CO_2CH_2CH_3$), 4.45 (s, 2H, NH_2, D_2O exchangeable), 5.04 (s,1H, pyran-H4), 7.17-7.29 (m, 4H, Ar-H), 7.39-7.50 (m, 3H, Ar-H), 7.56-7.59 (m, 1H, Ar-H), 7.67-7.70 (m, 2H, Ar-H), 7.71 (1H, s, pyrazole-H5); ^{13}C NMR (75 MHz; $CDCl_3$) δ_C 13.87 (CH_3), 18.58 (CH_3), 29.08 (pyran-C-4), 60.87 (pyran-C-5), 61.79 (CH_2), 104.26, 107.65, 111.33, 119.02, 119.39, 121.32, 123.08, 124.41, 125.76, 127.02, 127.90, 128.76, 129.55, 139.76, 142.55, 150.36, 155.00, 156.56, 157.81 (aromatic-C), 166.02 (CO); MS, m/z (%): 466 $[M]^+$ (3), 465 $[M]^{-1}$ (3), 77 $[C_6H_5]^+$ (100); Anal. For $C_{27}H_{22}N_4O_4$ (466.49): Calcd. C, 69.52; H, 4.75; N, 12.01; Found: C, 69.81; H, 4.93; N, 12.21.

4.1.4. 2-Amino-4-(3-(benzofuran-2-yl)-1-phenyl-1H-pyrazol-4-yl)-7-hydroxy-4H-chromene- 3-carbonitrile (6)

A mixture of compound **2** (0.68 g, 0.002 mol) and resorcinol (0.22 g, 0.002 mol) in absolute ethanol (20 mL) containing 2-3 drops of piperidine was refluxed for 1 h. The formed precipitate during heating was filtered, dried and recrystallized from ethanol to give the title compound **6**.

Yield 57%, mp. 252-254°C, yellow powder; IR (KBr, cm^{-1}): 3325, 3204, 3135 (OH, NH_2), 3060 (CH-arom.), 2197 (CN); ^{1}H NMR (300 MHz; DMSO-d_6) δ_H 5.21 (s, 1H, pyran-H4), 6.41-6.46 (m, 2H, Ar-H), 6.83-6.87 (m, 3H, Ar-H), 7.19 (s, 1H, OH, D_2O exchangeable), 7.24-7.36 (m, 4H, NH_2, D_2O exchangeable, Ar-H), 7.54 (t, 2H, ^3J = 8.1 Hz, Ar-H), 7.63 (t, 2H, ^3J = 8.7 Hz, Ar-H), 7.95 (d, 2H, ^3J = 7.5 Hz, Ar-H), 8.61 (1H, s, pyrazole-H5); ^{13}C NMR (75 MHz; DMSO-d_6) δ_C 30.73 (Chromene-C4), 55.84 (Chromene-C3), 102.61, 103.90, 111.71, 112.67, 113.30, 118.74, 121.41, 121.72, 123.75, 125.06, 127.21, 127.39, 128.56, 129.43, 130.09, 130.16, 139.56, 141.74, 149.44, 150.50, 154.56, 157.60, 160.70 (aromatic-C); MS, m/z (%): 446 $[M]^+$ (5), 429 $[M\text{-}OH]^+$ (42), 77 $[C_6H_5]^+$ (100); Anal. For $C_{27}H_{18}N_4O_3$ (446.46): Calcd. C, 72.64; H, 4.06; N, 12.55; Found: C, 72.92; H, 4.27; N, 12.26.

4.1.5. 2-Amino-4-(3-(benzofuran-2-yl)-1-phenyl-1H-pyrazol-4-yl)-5,6,7,8-tetrahydro-7,7-dimethyl-5-oxo-4H-chromene-3-carbonitrile (7)

A mixture of compound **2** (0.68 g, 0.002 mol) and dimedone (0.28 g, 0.002 mol) in absolute ethanol (20 mL) containing 2-3 drops of piperidine was stirred overnight at room temperature. The formed precipitate was filtered, dried, and recrystallized from ethanol to give the target compound **7**.

Yield 71%, mp. 264-266°C, white powder; IR (KBr, cm^{-1}): 3325, 3211 (NH_2), 3056 (CH-arom.), 2959, 2927, 2870 (CH-aliph.), 2189 (CN); ^{1}H NMR (300 MHz; DMSO-d_6) δ_H 0.64 (s, 3H, CH_3), 0.93 (s, 3H, CH_3), 1.97-2.02 (m, 1H, CH_2), 2.14-2.26 (m, 2H, CH_2), 2.46 (br.s, 1H, CH_2), 4.69 (s, 1H, pyran-H4), 6.99 (s, 2H, NH_2, D_2O exchangeable), 7.25-7.32 (m, 4H, Ar-H), 7.49 (t, 2H, ^3J = 7.8 Hz, Ar-H), 7.64 (t, 2H, ^3J = 7.8 Hz, Ar-H), 7.89 (d, 2H, ^3J = 7.8 Hz, Ar-H), 8.53 (s, 1H, pyrazole-H5); ^{13}C NMR (75 MHz; DMSO-d_6) δ_C 26.59 ((chromene-C4), 26.97 (CH_3), 28.86 (CH_3), 32.00 (chromene-C7), 50.56 (CH_2), 57.96 (CH_2), 104.17, 111.69, 112.02, 118.63, 120.44, 121.70, 123.68, 124.97, 126.728, 127.08, 128.71, 129.20, 130.10, 139.55, 141.67, 150.62, 154.68, 159.11, 163.01 (aromatic-C), 196.34 (CO); MS, m/z (%): 476 $[M]^+$ (3), 410 $[C_{24}H_{18}N_4O3]^+$ (58), 326 $[C_{21}H_{16}N_3O]^+$ (85), 66 $[C_5H_6]^+$ (100); Anal. For $C_{29}H_{24}N_4O_3$ (476.53): Calcd. C, 73.09; H, 5.08; N, 11.76; Found: C, 73.34; H, 5.28; N, 11.54.

 doi:10.20944/preprints202408.1792.v2

4.1.6. 6-Amino-4-(3-(benzofuran-2-yl)-1-phenyl-1H-pyrazol-4-yl)-3-methyl-1,4-dihydropyrano[2,3-c]pyrazole-5-carbonitrile (8)

A mixture of compound **2** (0.68 g, 0.002 mol) and 3-methyl-1*H*-pyrazol-5(4*H*)-one (0.20 g, 0.002 mol) in absolute ethanol (20 mL) containing 2-3 drops of piperidine was stirred at room temperature overnight. The formed precipitate was filtered, dried, and recrystallized from ethanol to give the target compound **8**.

Yield 75%, mp. 226-228°C, white powder; IR (KBr, cm^{-1}): 3393, 3306, 3176 (NH, NH_2), 3054 (CH-arom.), 2922, 2858 (CH-aliph.), 2186 (CN); ^{1}H NMR (300 MHz; DMSO-d_6) δ_H 1.83 (3H, s, CH_3), 5.17 (1H, s, pyran-H4), 6.89 (2H, s, NH_2, D_2O exchangeable), 7.21 (s,1H, Ar-H), 7.24-7.37 (m, 3H, Ar-H), 7.53 (t, 2H, ^3J = 7.95 Hz, Ar-H), 7.64 (t, 2H, ^3J = 7.8 Hz, Ar-H), 7.96 (d, 2H, ^3J = 7.5 Hz, ^4J = 1.2 Hz, Ar-H), 8.60 (1H, s, pyrazole-H5), 12.00 (1H, s, NH, D_2O exchangeable); ^{13}C NMR (75 MHz; DMSO-d_6) δ_C 10.25 (CH_3), 27.06 (pyran-C4), 56.93 (pyran-C3), 97.45 (CN), 104.03, 111.79, 118.69, 121.53, 121.66, 123.72, 125.01, 125.81, 127.16, 128.55, 129.22, 129.23, 130.13, 136.02, 139.57, 141.81, 150.51, 154.53, 155.34, 161.61, 171.66 (aromatic-C); MS, m/z (%): 434 $[M]^+$ (5), 368 $[C_{22}H_{16}N_4O_2]^+$ (100); Anal. For $C_{25}H_{18}N_6O_2$ (434.45): Calcd. C, 69.11; H, 4.18; N, 19.34; Found: C, 69.32; H, 4.35; N, 19.16.

4.1.7. 8-(3-(Benzofuran-2-yl)-1-phenyl-1H-pyrazol-4-yl)-6-oxo-1,3,4,6-tetrahydro-2H-pyrido[1,2-b][1,2,4]triazine-7,9-dicarbonitrile (9)

A mixture of compound **4** (0.87 g, 0.002 mol) and 1,2-dibromoethane (0.18 mL, 0.002 mol) in pyridine (15 mL) was refluxed for 6 h. The reaction mixture was poured onto ice/cold water; the formed precipitate was filtered, dried, and recrystallized from ethanol to give the title compound **9**.

Yield 93%, mp. 238-240°C, white powder; IR (KBr, cm^{-1}): 3189, 3127 (2NH), 3049 (CH-arom.), 2922, 2854 (CH-aliph.), 2213 (2CN), 1639 (C=O); ^{1}H NMR (300 MHz; DMSO-d_6) δ_H 2.07 (m, 2H, CH_2), 2.43 (m, 2H, CH_2), 6.94 (s, 1H, Ar-H), 7.24 (d, 1H, ^3J = 7.5 Hz, Ar-H), 7.32 (t, 2H, ^3J = 7.5 Hz, Ar-H), 7.42 (t, 1H, ^3J = 7.2 Hz, Ar-H), 7.58-7.67 (m, 3H, Ar-H), 7.98-8.06 (m, 2H, Ar-H), 9.05 (1H, s, pyrazole-H5), 9.09 (s, 1H, NH, D_2O exchangeable); ^{13}C NMR (75 MHz; DMSO-d_6) δ_C 31.18 (CH_2), 71.45 (CH_2), 78.49, 85.06, 105.14, 111.70, 116.93, 117.18, 119.01, 122.06, 123.73, 125.5113, 127.58, 127.74, 128.67, 130.15, 130.33, 139.28, 141.72, 142.95, 146.06, 148.78, 152.94, 154.46, 156.34 (aromatic-C), 161.64 (CO); MS, m/z (%): 458 $[M]^{-1}$ (16), 457 $[M]^{-2}$ (20), 433 $[M-C_2H_2]^+$ (40), 51 $[C_4H_3]^+$ (100); Anal. For $C_{26}H_{17}N_7O_2$ (459.46): Calcd. C, 67.97; H, 3.73; N, 21.34; Found: C, 67.64; H, 3.51; N, 21.58.

4.1.8. 3-Acetyl-7-(3-(benzofuran-2-yl)-1-phenyl-1H-pyrazol-4-yl)-3,5-dihydro-2-methyl-5-oxo-[1,2,4]triazolo[1,5-a]pyridine-6,8-dicarbonitrile (10)

A mixture of compound **4** (0.87 g, 0.002 mol) and acetic anhydride (10 mL) was refluxed for 1 h. Upon cooling, the formed precipitate was filtered, dried, and recrystallized from acetic acid to give the title compound **10**.

Yield 74%, mp. >300°C, yellow powder; IR (KBr, cm^{-1}): 3051 (CH-arom.), 2925, 2846 (CH-aliph.), 2223 (2CN), 1671 (2C=O); ^{1}H NMR (300 MHz; DMSO-d_6) δ_H 1.92 (s, 3H, CH_3), 2.09 (s, 3H, CH_3), 7.04 (s, 1H, Ar-H), 7.26 (t, 1H, ^3J = 7.65 Hz, Ar-H), 7.35 (t, 1H, ^3J = 8.1 Hz, Ar-H), 7.44 (t, 1H, ^3J = 7.35 Hz, Ar-H), 7.59-7.65 (m, 4H, Ar-H), 8.02 (d, 2H, ^3J = 7.8 Hz, Ar-H), 9.09 (s, 1H, pyrazole-H5); ^{13}C NMR (75 MHz; DMSO-d_6) δ_C 21.567 (CH_3), 31.19 (CH_3), 77.17, 87.08, 105.39, 111.78, 116.19, 116.62, 117.83, 119.12, 122.04, 123.79, 125.59, 127.87, 128.70, 130.37, 139.24, 141.73, 147.31, 148.60, 151.33, 154.52, 155.66 (aromatic-C), 158.98 (CO); MS, m/z (%): 498 $[M]^{-1}$ (3), 418 $[C_{24}H_{14}N_6O_2]^+$ (32), 56 $[C_4H_8]^+$ (100); Anal. For $C_{28}H_{17}N_7O_3$ (499.48): Calcd. C, 67.33; H, 3.43; N, 19.63; Found: C, 67.52; H, 3.14; N, 19.80.

4.1.9. 7-(3-(Benzofuran-2-yl)-1-phenyl-1H-pyrazol-4-yl)-1,2,3,5-tetrahydro-2-(substituted)-5-oxo-[1,2,4]triazolo[1,5-a]pyridine-6,8-dicarbonitrile 11a-d

A mixture of compound **4** (0.87 g, 0.002 mol) and the appropriate aldehyde derivatives, namely 3,4,5-trimethoxybenzaldehyde, 4-chlorobenzaldehyde, 5-methylfuran-2-carbaldehyde, and/or thiophene-2-carbaldehyde (0.002 mol), in acetic acid (20 mL), was refluxed for 6-8 h. After cooling, the formed precipitate was filtered, dried, and recrystallized from acetic acid to give the title compounds **11a-d,** respectively.

 doi:10.20944/preprints202408.1792.v2

4.1.10.1. 7-(3-(Benzofuran-2-yl)-1-phenyl-1H-pyrazol-4-yl)-1,2,3,5-tetrahydro-2- (3,4,5-trimethoxyphenyl)-5-oxo-[1,2,4]triazolo[1,5-a]pyridine-6,8-dicarbonitrile (11a)

Yield 83%, mp. 297-299°C, white powder; IR (KBr, cm^{-1}): 3299, 3214 (2NH), 3067 (CH-arom.), 2942, 2832 (CH-aliph.), 2221 (2CN), 1665 (C=O); ^{1}H NMR (300 MHz; DMSO-d_6) δ_H 3.79 (s, 3H, OCH_3), 3.89 (s, 6H, 2(OCH_3)), 7.27-7.48 (m, 6H, Ar-H), 7.63 (t, 2H, *J* = 7.95 Hz, Ar-H), 7.71 (d, 2H, *J* = 7.80 Hz, Ar-H), 8.03 (d, 2H, *J* = 7.80 Hz, Ar-H), 8.56 (br, 2H, 2NH, D_2O exchangeable), 8.90 (s, 1H, triazole-H3), 9.13 (s, 1H, pyrazole-H5); ^{13}C NMR (75 MHz; DMSO-d_6) δ_C 56.65, 60.82, 90.26, 107.80, 115.75, 115.77, 119.21, 122.18, 125.63, 125.70, 125.74, 125.76, 125.79, 126.23, 126.38, 126.73, 127.10, 127.39, 127.40, 127.73, 128.77, 130.43, 140.88, 146.02, 147.29, 153.53, 154.61, 156.86, 158.59, 159.06, 159.42 (aromatic-C); MS, m/z (%): 611 $[M]^+$ (74), 610 $[M]^{-1}$ (29), 236 $[C_{11}H_{14}N_3O_3]^+$ (100); Anal. For $C_{34}H_{25}N_7O_5$ (611.62): Calcd. C, 66.77; H, 4.12; N, 16.03; Found: C, 66.41; H, 4.33; N, 16.35.

4.1.11.2. 7-(3-(Benzofuran-2-yl)-1-phenyl-1H-pyrazol-4-yl)-2-(4-chlorophenyl)-1,2,3,5-tetrahydro-5-oxo-[1,2,4]triazolo[1,5-a]pyridine-6,8-dicarbonitrile (11b)

Yield 61%, mp. 221-223°C, white powder; IR (KBr, cm^{-1}): 3299, 3192 (2NH), 3055 (CH-arom.), 2218 (2CN), 1676 (C=O); ^{1}H NMR (300 MHz; DMSO-d_6) δ_H 7.28-7.32 (m, 2H, Ar-H), 7.38 (t, 1H, *J* = 7.2 Hz, Ar-H), 7.45 (t, 1H, *J* = 7.35 Hz, Ar-H), 7.45 (t, 2H, *J* = 7.95 Hz, Ar-H), 7.68 (d, 4H, *J* = 8.4 Hz, Ar-H), 7.99 (d, 2H, *J* = 7.8 Hz, Ar-H), 8.09 (d, 2H, *J* = 8.7 Hz, Ar-H), 8.62 (br., 2H, 2NH, D_2O exchangeable), 9.07 (s, 1H, triazole-CH), 9.12 (s, 1H, pyrazole-H5) ; ^{13}C NMR (75 MHz; DMSO-d_6) δ_C 76.50, 89.11, 105.76, 111.92, 111.95, 115.74, 116.65, 119.24, 122.07, 123.91, 123.94, 125.71, 128.07, 128.09, 128.76, 129.57, 130.42, 131.15, 132.05, 138.54, 139.12, 148.35, 154.63, 156.81, 161.98, 170.87, 171.92 (aromatic-C); MS, m/z (%): 555 $[M]^+$ (3), 556 $[M]^{+1}$ (2), 418 $[C_{24}H_{14}N_6O_2]^+$ (58), 137 $[C_7H_4ClN]^+$ (100); Anal. For $C_{31}H_{18}ClN_7O_2$ (555.97): Calcd. C, 66.97; H, 3.26; N, 17.64; Found: C, 67.19; H, 3.42; N, 17.39.

5.1.12.3. 7-(3-(Benzofuran-2-yl)-1-phenyl-1H-pyrazol-4-yl)-1,2,3,5-tetrahydro-2-(5- methylfuran-2-yl)-5-oxo-[1,2,4]triazolo[1,5-a]pyridine-6,8-dicarbonitrile (11c)

Yield 85%, mp. 217-219°C, grey powder; IR (KBr, cm^{-1}): 3196, 3125 (2NH), 3062 (CH-arom.), 2929, 2850 (CH-aliph.), 2217 (2CN), 1664 (C=O); ^{1}H NMR (300 MHz; DMSO-d_6) δ_H 2.46 (s, 3H, CH_3), 6.51 (d, 1H, *J* = 6.7 Hz, furan-H), 6.95 (s, 1H, furan-H), 7.17 (s, 1H, Ar-H), 7.24-7.47 (m, 4H, Ar-H), 7.62-7.69 (m, 2H, Ar-H), 7.99-8.01 (m, 2H, Ar-H), 8.44, 8.58 (2br., 2H, 2NH, D_2O exchangeable), 8.68 (s, 1H, pyrazole-H5), 9.11 (s, 1H, triazole-CH); ^{13}C NMR (75 MHz; DMSO-d_6) δ_C 14.28 (CH_3), 69.02, 76.39, 105.01, 111.90, 115.79, 115.86, 119.20, 122.05, 122.10, 123.74, 123.90, 125.52, 125.69, 126.31, 127.63, 128.71, 130.40, 139.10, 141.60, 146.32, 154.61, 154.73, 157.17, 159.20, 162.93, 165.01 (aromatic-C); MS, m/z (%): 525 $[M]^+$ (21), 526 $[M]^{+1}$ (10), 82 $[C_5H_6O]^+$ (100); Anal. For $C_{30}H_{19}N_7O_3$ (525.52): Calcd. C, 68.57; H, 3.64; N, 18.66; Found: C, 68.73; H, 3.49; N, 18.40.

5.1.13.4. 7-(3-(Benzofuran-2-yl)-1-phenyl-1H-pyrazol-4-yl)-1,2,3,5-tetrahydro-5-oxo-2-(thiophen-2-yl)-[1,2,4]triazolo[1,5-a]pyridine-6,8-dicarbonitrile (11d)

Yield 92%, mp. 194-196°C, grey powder; IR (KBr, cm^{-1}): 3214, 3136 (2NH), 3051 (CH-arom.), 2927, 2845 (CH-aliph.), 2219 (2CN), 1668 (C=O); ^{1}H NMR (300 MHz; DMSO-d$_6$) δ_H 7.17 (s, 1H, thiophene-H) 7.29-7.34 (4H, m, Ar-H), 7.59-7.68 (5H, m, Ar-H), 7.98-8.02 (3H, m, Ar-H, triazole-H3), 8.58 (2H, 2s, 2NH, D_2O exchangeable), 9.10 (1H, s, pyrazole-H5), 9.14 (s, 1H, triazole-CH); ^{13}C NMR (75 MHz; DMSO-d$_6$) δ_C 75.98, 88.18, 105.39, 115.89, 119.22, 120.68, 122.06, 123.91, 125.70, 128.04, 128.63, 130.41, 139.12, 141.56, 142.51, 148.51, 151.39, 152.45, 156.89, 161.69 (aromatic-C), 169.12 (CO); MS, m/z (%): 527 $[M]^+$ (42), 528 $[M^{+1}]^{+1}$ (41), 443 $[M\text{-}C_4H_4S]^+$ (45), 77 $[C_6H_5]^+$ (100); Anal. For $C_{29}H_{17}N_7O_2S$ (527.56): Calcd. C, 66.02; H, 3.25; N, 18.59; S, 6.08; Found: C, 66.28; H, 3.41; N, 18.72; S, 6.22.

4.2. Biological Evaluation

4.2.1. In Vitro Antimicrobial Activity

The antibacterial screening bioassay was made by the agar well diffusion method using Mueller-Hinton agar (Lab M Limited, Bury, Lancashire, UK), then the plates were transferred to refrigerator for 1 h at 4 °C [49-52]. More detailed descriptions are available in the file of Supporting Information.

 doi:10.20944/preprints202408.1792.v2

4.2.2. Human Red Blood Cell Stabilization Method

The human red blood cell (HRBC) membrane stabilization method was used to study the *in vitro* anti-inflammatory activity of the new samples [69]. More detailed descriptions are available in the file of Supporting Information.

4.2.3. DPPH Radical Scavenging Assay

The DPPH (1–diphenyl–2–picrylhydrazyl) scavenging activity of the sample was determined quantitatively according to the reported method [70, 71]. More detailed descriptions are available in the file of Supporting Information.

4.2.4. E. coli DNA Gyrase B Suppression Effect

The *in vitro* enzyme inhibition assessment was performed against *E. coli* DNA gyrase according to the optimized protocol by the manufacturer [62-64]. More detailed descriptions are available in the file of Supporting Information.

4.2.5. In Vitro Cytotoxicity Assay

The cytotoxic effect of test samples using WI38 cells was evaluated by MTT assay [64]. Commercially available kit for *in vitro* toxicology MTT based assay, Sigma was used. More detailed descriptions are available in the file of Supporting Information.

4.2.6. Molecular Docking

Molecular Operating Environment (MOE, 2019.0102) was used for the docking study. By using the steepest descent technique with the MMFF94x force field until the RMSD gradient of 0.1 kcal.mol^{-1}Å^{-1} was reached, energy-minimized structures were created. The crystal structure of DNA gyrase enzyme complexed with novobiocin was obtained from the protein data bank with PDB ID: **4URO**. In the same way, the x-ray crystallographic structure of topoisomerase IV with the co-crystallized ligand; novobiocin; was downloaded (PDB ID: **1S14**). Despite docking software's capacity to identify potential binding modes between a ligand and its target, it is still an unreliable method that requires constant verification [66-68].

Supplementary Materials: The following supporting information can be downloaded at the website of this paper posted on Preprints.org.

Funding: This research is supported by Researchers Supporting Project number (RSPD2024R930), King Saud University, Riyadh, Saudi Arabia.

Institutional Review Board Statement: Not applicable.

Informed Consent Statement: Not applicable.

Data Availability Statement: Data will be made available on request. S.S.A., M.M.A., Y.M.S., H.M.A., A.N.E., M.K.A., H.M.A., S.H.A.

Conflicts of Interest: The authors declare no conflict of interest.

Declaration of Competing Interest: The authors declare that they have no known competing financial interests or personal relationships that could have appeared to influence the work reported in this paper.

Acknowledgments National Research Center & Prairie View University Faculty startup funds 552509-00018.

Sample Availability: Samples of the compounds are not available from the authors.

References

1. Xue, W.; Zuo, X.; Zhao, X.; Wang, X.; Zhang, X.; Xia, J.; Cheng, M.; Yang, H. Bioisosteric replacement strategy leads to novel DNA gyrase B inhibitors with improved potencies and properties. *Bioorg. Chem.* **2024**, 147, 107314, https://doi.org/10.1016/j.bioorg.2024.107314

2. Princiotto, S.; Casciaro, B.; Temprano, A.G.; Musso, L.; Sacchi, F.; Loffredo, M.R.; Cappiello, F., Sacco, F.; Raponi, G.; Fernandez, V.P.;Iucci, T. The antimicrobial potential of adarotene derivatives against Staphylococcus aureus strains. *Bioorg. Chem.* **2024**, 107227, https://doi.org/10.1016/j.cmi.2015.10.010
3. Vouga, M.; Greub, G. Emerging bacterial pathogens: the past and beyond. *Clinical Microbiology and Infection (CMI)*. 2016, 22(1):12-21. https://doi.org/10.1016/j.cmi.2015.10.010
4. Du, M.; Xuan, W.; Zhen, X..; He, L.; Lan, L.; Yang, S.; Wu, N.; Qin, J.; Qin, J.; Lan, J.; Lu, H.; Liang, C.; Li, Y.; Hamblin, M.R.; Huang, L. Antimicrobial photodynamic therapy for oral Candida infection in adult AIDS patients: A pilot clinical trial Photodiagn. *Photodyn. Ther.* **2021**, 34, 102310, https://doi.org/10.1016/j.pdpdt.2021.102310
5. Chalkha, M.; Akhazzane, M.; Moussaid, F.Z.; Daoui, O.; Nakkabi A.; Bakhouch, M.; Chtita, S.; Elkhattabi, S.; Housseini, A.I.; El Yazidi, M. Design, synthesis, characterization, in vitro screening, molecular docking, 3D-QSAR, and ADME-Tox investigations of novel pyrazole derivatives as antimicrobial agents. *New J Chem.* **2022**, 46(6), 2747-60, DOI: 10.1039/d1nj05621b
6. Tang, K.W.; Millar, B.C.; Moore, J.E. Antimicrobial Resistance (AMR). *Br J Biomed Sci.* **2023**, 80, 11387, https://doi.org/10.3389/bjbs.2023.11387
7. Zhang, N.; Ma, S. Recent development of membrane-active molecules as antibacterial agents. *Eur. J. Med. Chem.* **2019**, 184, 111743, https://doi.org/10.1016/j.ejmech.2019.111743
8. Richa, K.; Namarata, S.; Negi, A.; Kumar, E.; Zangrando, R.; Saini, V. Synthesis, characterization and utility of a series of novel copper(II) complexes as excellent surface disinfectants against nosocomial infections. *Dalton Trans.* **2021**, 50, 13699–13711, DOI: 10.1039/d1dt00199j
9. Founou, R.C.; Blocker, A.J.; Noubom, M.; Tsayem, C.; Choukem, S.P.; Dongen, M.V.; *et al.* The COVID-19 Pandemic: a Threat to Antimicrobial Resistance Containment. *Future Sci*. **2021**, 7(8), FSO736, doi:10.2144/fsoa-2021-0012
10. Patel, P.; Shakya R.; Asati, V.; Kurmi, B.D.; Verma, S.K.; Gupta, G.D.; Rajak, H. Furan and benzofuran derivatives as privileged scaffolds as anticancer agents: SAR and docking studies (2010 to till date). *J. Mol. Struct.* **2024**, 1299,137098, https://doi.org/10.1016/j.molstruc.2023.137098
11. Cebeci, Y.U.; Batur, Ö.Ö.; Boulebd, H. Design, synthesis, theoretical studies, and biological activity evaluation of new nitrogen-containing poly heterocyclic compounds as promising antimicrobial agents. *J. Mol. Struct.* **2024**, 1299, 137115, https://doi.org/10.1016/j.molstruc.2023.137115
12. Dawood, K.M. An update on benzofuran inhibitors: a patent review. *Expert Opin. Ther. Pat.* **2019**, 29 (11), 841–870, https://doi.org/10.1080/13543776.2019.1673727
13. Abbas, A.A.; Dawood, K.M. Anticancer therapeutic potential of benzofuran scaffolds. *RSC Adv.* **2023**, 13 (16), 11096–11120, DOI: 10.1039/d3ra01383a
14. Khanam, H. Bioactive Benzofuran derivatives: A review. *Eur j med chem.* **2015**, 97, 483-504, https://doi.org/10.1016/j.ejmech.2014.11.039
15. Nevagi, R.J.; Dighe, S.N.; Dighe, S.N. Biological and medicinal significance of benzofuran. *Eur. J. Med. Chem*. **2015**, 97, 561–581, https://doi.org/10.1016/j.ejmech.2014.10.085
16. Saeed, S.; Zahoor, A.F.; Kamal, S.; Raza, Z.; Bhat, M.A. Unfolding the antibacterial activity and acetylcholinesterase inhibition potential of benzofuran-triazole hybrids: Synthesis, antibacterial, acetylcholinesterase inhibition, and molecular docking studies. *Molecules.* **2023**, 28(16), 6007, https://doi.org/10.3390/molecules28166007

17. El-Zahar, M.I.; Abd El-Karim, S.S.; Anwar, M.M. Synthesis and cytotoxicity screening of some novel benzofuranoyl-pyrazole derivatives against liver and cervix carcinoma cell line. *S. Afr. J. Chem.* **2009**, 62, 189-199.
18. Abd El-Karim, S.S.; Anwar, M.M.; Mohamed, N.A.; Nasr, T.; Elseginy, S.A. Design, synthesis, biological evaluation and molecular docking studies of novel benzofuran–pyrazole derivatives as anticancer agents. *Bioorg. Chem*. **2015**, 63, 1–12, https://doi.org/10.1016/j.bioorg.2015.08.006.
19. Anwar, M.M.; Abd El-Karim, S.S.; Mahmoud, A.H.; Amr, A.G.E.; Mohamed, A. A. A Comparative study of the anticancer activity and PARP-1 inhibiting Effect of benzofuran–pyrazole scaffold and its nano-sized particles in human breast cancer cells. *Molecules*. **2019**, 24, 2413, https://doi.org/10.3390/molecules24132413
20. Siddiqui, N.J.; Idrees. M. Condensation-cyclodehydration of 2,4-dioxobutanoates: Synthesis of new esters of pyrazoles and isoxazoles and their antimicrobial screening. *Der Pharm. Chem.* **2014**, 6, 406-410, http://derpharmachemica.com/vol6-iss6/DPC-2014-6-6-406-410.pdf
21. Liu, J.B.; Jiang, F.Q.; Jiang, X.Z.; Zhang, W.; Liu, J.J.; Liu, W.L.; Fu. L. Synthesis and antimicrobial evaluation of 3-methanone-6-substitutedbenzofuran derivatives. *Eur. J. Med. Chem.* **2012**, 54 879-886, https://doi.org/10.1016/j.ejmech.2012.05.013
22. Ashok, D.; Srinivas, G.V.; Kumar, A.; Gandhi. D.M. Microwave-assisted synthesis and evaluation of indole based benzofuran Scaffolds as antimicrobial and antioxidant Agents. *Russ. J. Bioorg. Chem.* **2016**, 42, 560-566.
23. Venkatesh, T.; Bodke, Y. D.; Joy, M.N.; Dhananjaya, B.L.; Venkataraman. S. Synthesis of some benzofuran derivatives containing pyrimidine moiety as potent antimicrobial agents. *Iran. J. Pharm. Res.* **2018**, 17, 75-86.
24. Yu, Z.; Shi, G.; Sun, Q.; Jin, H.; Teng, Y.; Tao, K.; Zhou, G.; Liu, W.; Wen, F.; Hou. T. Design, synthesis and in vitro antibacterial/antifungal evaluation of novel 1-ethyl-6-fluoro-1,4-dihydro-4-oxo-7(1-piperazinyl)quinoline-3-carboxylic acid derivatives. *Eur. J. Med. Chem.* **2009**, 44, 4726-4733, https://doi.org/10.1016/j.ejmech.2009.05.028
25. Chougala, B.M.; Shastri, S.L.; Holiyachi, M.; Shastri, L.A.; More, S.S.; Ramesh. K.V. Synthesis, anti-microbial and anti-cancer evaluation study of 3-(3-benzofuranyl)-coumarin derivatives. *Med. Chem. Res.* **2015**, 24, 4128-4136, DOI 10.1007/s00044-015-1449-y
26. Wang, Y.; Chen, F.; Di, H.; Xu, Y.; Xiao, Q.; Wang, X.; Wei, H.; Lu, Y.; Zhang, L.; Zhu, J.; Sheng, C.; Lan, L.; Li. J. Discovery of potent benzofuran-derived diapophytoene desaturase (CrtN) inhibitors with enhanced oral bioavailability for the treatment of methicillin-resistant staphylococcus aureus (MRSA) infections. *J. Med. Chem.* **2016**, 59, 3215-3230, DOI:10.1021/acs.jmedchem.5b01984J
27. Venkateshwarlu, T.; Nath, A.R.; Chennapragada. K.P. Synthesis and antimicrobial activity of novel benzo[b]furan derivatives. *Der Pharm. Chem.* **2013**, 5, 229-234, http://derpharmachemica.com/archive.html
28. Verma, R.; Verma S.K.; Rakesh, K.P.; Girish, Y.R.; Ashrafizadeh, M.; Kumar, K.S.; Rangappa, K.S. Pyrazole-based analogs as potential antibacterial agents against methicillin-resistance staphylococcus aureus (MRSA) and its SAR elucidation. *Eur j med chem.* **2021**, 212, 113134, https://doi.org/10.1016/j.ejmech.2020.113134
29. Ibrahim, S.A.; Fayed, E.A.; Rizk, H.F.;Desouky, S.E.; Ragab, A. Hydrazonoyl bromide precursors as DHFR inhibitors for the synthesis of bis-thiazolyl pyrazole derivatives; antimicrobial activities, antibiofilm, and drug combination studies against MRSA. *Bioorg chem.* **2021**, 116, 105339, https://doi.org/10.1016/j.bioorg.2021.105339

30. Laamari, Y.; Fawzi, M.; Hachim, M.E.; Bimoussa, A.; Oubella, A.; Ketatni, E.M.; Saadi, M.; El Ammari, L.; Itto, M.Y.; Morjani, H.; Khouili, M. Synthesis, characterization and cytotoxic activity of pyrazole derivatives based on thymol. *J Mol Struct*. **2024**, 1297, 136864, https://doi.org/10.1016/j.molstruc.2023.136864
31. Mortada, S.; Karrouchi, K.; Hamza, E.H.; Oulmidi, A.; Bhat, M.A.; Mamad, H.; Aalilou ,Y.; Radi, S.; Ansar, M.H.; Masrar, A.; Faouzi, M.E. Synthesis, structural characterizations, *in vitro* biological evaluation and computational investigations of pyrazole derivatives as potential antidiabetic and antioxidant agents. *Sci Rep.* **2024**, 14(1), 1312. https://doi.org/10.1038/s41598-024-51290-6
32. Singh, S.; Tahlan, S.; singh, K.; Verma, P.K. Synthetic Update on Antimicrobial Potential of Novel Pyrazole Derivatives: A Review. *Curr. Org. Chem*. **2024**, DOI: 10.2174/0113852728292094240216045039
33. Mohamed, H.A.; Abdel-Latif, E.; Abdel-Wahab, B.F.; Awad, G.E. Novel antimicrobial agents: fluorinated 2-(3-(benzofuran-2-yl) pyrazol-1-yl) thiazoles. *Int. J. Med. Chem.* **2013**, 2013, DOI: 10.1155/2013/986536
34. Rangaswamy, J.; Kumar, H.V.; Harini, S.T.; Naik, N. Synthesis of benzofuran based 1, 3, 5-substituted pyrazole derivatives: As a new class of potent antioxidants and antimicrobials-A novel accost to amend biocompatibility. *Bioorg. Med. Chem. lett.* **2012**, 22(14), 4773-7, https://doi.org/10.1016/j.bmcl.2012.05.061
35. Abd El-Karim, S.S.; Mahmoud, A.H.; Al-Mokaddem, A.K.; Ibrahim, N.E.; Alkahtani, H.M.; Zen, A.A.; Anwar, M.M. Development of a New Benzofuran–Pyrazole–Pyridine-Based Molecule for the Management of Osteoarthritis. *Molecules* **2023**, 28, 6814, https://doi.org/10.3390/molecules28196814
36. Chen, Y.; Chen, R.; Yuan, R.; Huo, L.; Gao, H.; Zhuo, Y.; Chen, X.; Zhang, C.; Yang, S. Discovery of New Heterocyclic/Benzofuran Hybrids as Potential Anti-Inflammatory Agents: Design, Synthesis, and Evaluation of the Inhibitory Activity of Their Related Inflammatory Factors Based on NF-κB and MAPK Signaling Pathways. *Int. J. Mol. Sci.* **2023**, 24(4), 3575, https://doi.org/10.3390/ijms24043575
37. Rangaswamy, J.; Kumar, H.V.; Harini, S.T.; Naik, N. Functionalized 3-(benzofuran-2-yl)-5-(4-methoxyphenyl)-4, 5-dihydro-1H-pyrazole scaffolds: A new class of antimicrobials and antioxidants. *Arab. J. Chem.* **2017**, 10, S2685-96, DOI: 10.1016/j.arabjc.2013.10.012
38. Rangaswamy, J.; Kumar, H.V.; Harini, S.T.; Naik, N. Synthesis of benzofuran based 1, 3, 5-substituted pyrazole derivatives: As a new class of potent antioxidants and antimicrobials-A novel accost to amend biocompatibility. *Bioorg. Med.* Chem. Let. **2012**, 22(14), 4773-7, https://doi.org/10.1016/j.bmcl.2012.05.061
39. Pommier, Y.; Leo, E.; Zhang, H.; Marchand, C. DNA topoisomerases and their poisoning by anticancer and antibacterial drugs. Chem. Biol. **2010**, 17, 421–433, https://doi.org/10.1016/j.chembiol.2010.04.012
40. Toyting, J.; Miura, N.; Utrarachkij, F.; Tanomsridachchai, W.; Belotindos, L.P.; Suwanthada, P.; Kapalamula, T.F.; Kongsoi, S.; Koide, K.; Kim, H.; Thapa, J. Exploration of the novel fluoroquinolones with high inhibitory effect against quinolone-resistant DNA gyrase of Salmonella Typhimurium. *Microbiol. Spectr.* **2023**, https://doi.org/10.1128/spectrum.01330-23 e01330-23
41. Hooper, D.C.; Jacoby, G.A. Topoisomerase inhibitors: fluoroquinolone mechanisms of action and resistance, Cold Spring Harb. *Perspect. Med.* **2016**, 6, https://doi. org/10.1101/cshperspect.a025320
42. Kerru, N.; Gummidi, L.; Maddila, S.; Gangu, K.K.; Jonnalagadda, S.B. A review on recent advances in nitrogen-containing molecules and their biological applications. *Molecules.* **2020**, 25(8), 1909, https://doi.org/10.3390/molecules25081909
43. Aatif, M.; Raza, M.A.; Javed, K.; Nashre-ul-Islam, S.M.; Farhan, M.; Alam, M.W. Potential nitrogen-based heterocyclic compounds for treating infectious diseases: a literature review. *Antibiotics*. **2022**, 11(12), 1750, https://doi.org/10.3390/antibiotics11121750
44. Egbujor, M.C.; Tucci, P.; Onyeije, U.C.; Emeruwa, C.N.; Saso, L. NRF2 Activation by Nitrogen Heterocycles: A Review. *Molecules.* **2023**, 28(6), 2751, https://doi.org/10.3390/molecules28062751

45. Egbujor, M.C.; Tucci, P.; Onyeije, U.C.; Emeruwa, C.N.; Saso, L. NRF2 Activation by Nitrogen Heterocycles: A Review. *Molecules*. **2023**, 28(6), 2751, https://doi.org/10.3390/molecules28062751
46. Peerzada, M.N.; Hamel, E.; Bai, R.; Supuran, C.T.; Azam, A. Deciphering the key heterocyclic scaffolds in targeting microtubules, kinases and carbonic anhydrases for cancer drug development. *Pharmacol. Ther.* **2021**, 225, 107860, https://doi. org/10.1016/j.pharmthera.2021.107860
47. Cebeci, Y.U.; Batur, Ö.Ö.; Boulebd, H. Design, synthesis, theoretical studies, and biological activity evaluation of new nitrogen-containing poly heterocyclic compounds as promising antimicrobial agents. *J Mol Struct*. **2024**, 1299, 137115, https://doi.org/10.1016/j.molstruc.2023.137115
48. Faleye, O.S.; Boya, B.R.; Lee, J.H.; Choi, I.; Lee, J. Halogenated Antimicrobial Agents to Combat Drug-Resistant Pathogens. *Pharmacol Rev.* **2024**, 76(1), 90-141, doi.org/10.1124/pharmrev.123.000863
49. Khalaf, H.S.; Naglah, A.M.; Al-Omar, M.A.; Moustafa, G.O.; Awad, H.M.; Bakheit, A.H. Synthesis, docking, computational studies, and antimicrobial evaluations of new dipeptide derivatives based on nicotinoylglycylglycine hydrazide, *Molecules*. **2020**, 25 (16), 3589, https://doi.org/10.3390/molecules25163589
50. Princiotto, S.; Casciaro, B.; Temprano, A.G.; Musso, L.; Sacchi, F.; Loffredo, M.R.; Cappiello, F.; Sacco, F.; Raponi, G.; Fernandez, V.P.; Iucci, T. The antimicrobial potential of adarotene derivatives against Staphylococcus aureus strains, *Bioorg Chem.* **2024**, 145, 107227, http://ejchem.journals.ekb.eg/
51. Gulcin, I.; Alici, H.A.; Cesur, M. Determination of *in vitro* antioxidant and radical scavenging activities of propofol. *Chem. Pharm. Bull.* **2005**, 53281–285, https://doi.org/10.1248/cpb.53.281.
52. Pervin, M.; Hasnat, M.A.; Lee, Y.M.; Kim, D.H.; Jo, J.E.; Lim, B.O. Antioxidant activity and acetylcholinesterase inhibition of grape skin anthocyanin (GSA). *Molecules*. **2014**, 19, 9403–9418, https://doi.org/10.3390/molecules28031057.
53. Lee, B.; Kim, J.; Kang, Y. M.; Lim, J.; Kim, Y.; Lee, M.; Ji-Hyun L., Young-Mog K., Myung-S., Min-Ho J., Chang-Bum A., Jae-Young J. Antioxidant activity and γ–aminobutyric acid (GABA) content in sea tangle fermented by Lactobacillus brevis BJ20 isolated from traditional fermented foods. *Food Chem.* **2010**, 122, 271–276, doi:10.1016/j.foodchem.2010.02.071
54. Üstündağ, H. The role of antioxidants in sepsis management: a review of therapeutic applications. *Eurasian Mol Biochem Sci.* **2023**, 2(2), 38-48.
55. Murugasan, N.; Vember, S.; Damodharan, C. Studies on erythrocyte membrane IV. vitro haemolytic activity of Oleander extract. *Toxicol Lett.* **1981**, 8, 33-38, https://doi.org/10.1016/0378-4274(81)90134-X
56. Chirumamilla, P.; Taduri, S. Assessment of in vitro anti-inflammatory, antioxidant and antidiabetic activities of Solanum khasianum Clarke. *Vegetos*. **2023**, 36(2), 575-82, https://doi.org/10.1007/s42535-022-00410-6
57. Shinde, U.A.; Phadke, A.S.; Nair, A.M.; Mungantiwar, A.A.; Dikshit, V.J.; Saraf, M.N. Studies on the anti-inflammatory and analgesic activity of Cedrus deodara (Roxb.) Loud. wood oil. *J. Ethnopharmacol.* **1999**, 65(1), 21-7, https://doi.org/10.1016/S0378-8741(98)00150-0
58. Oyedapo, O.O.; Akinpelu, B.A.; Akinwunmi, K.F.; Adeyinka, M.O.; Sipeolu, F.O. Red blood cell membrane stabilizing potentials of extracts of Lantana camara and its fractions. *International Journal of Plant Physiology and Biochemistry (IJPPB)*. **2010**, 2(4), 46-51. t http://www.academicjournals.org/ijppb
59. Chopade, S.G.; Kulkarni, K.S.; Kulkarni, A.D.; Topare, N.S. Solid heterogeneous catalysts for production of biodiesel from trans-esterification of triglycerides with methanol: a review. *Acta Chimica and Pharmaceutica Indica*. **2012**, 2(1), 8-14.

60. Hashem, H.E.; Amr, A.E.; Nossier, E.S.; Elsayed, E.A.; Azmy, E.M. Synthesis, antimicrobial activity and molecular docking of novel thiourea derivatives tagged with thiadiazole, imidazole and triazine moieties as potential DNA gyrase and topoisomerase IV inhibitors. *Molecules*. **2020**, 25(12), 2766, https://doi.org/10.3390/molecules25122766
61. Jakopin, Z.; Ilas, J.; Barancokova, M.; Brvar, M.; Tammela, P.; Dolenc, M.S.; Tomasic, T.; Kikelj, D. Discovery of substituted oxadiazoles as a novel scaffold for DNA gyrase inhibitors. *Eur. J. Med. Chem.* **2017**, 130, 171-184, https://doi.org/10.1016/j.ejmech.2017.02.046
62. Gjorgjieva, M.; Tomašič, T.; Barančokova, M.; Katsamakas, S.; Ilaš, J.; Tammela, P.; Mašič, L.P.; Kikelj, D. Discovery of benzothiazole scaffold-based DNA Gyrase B inhibitors. *J. Med. Chem*. **2016**, 59, 8941−8954, DOI: 10.1021/acs.jmedchem.6b00864
63. Mosmann, T. Rapid colorimetric assay for cellular growth and survival: application to proliferation and cytotoxicity assays. *J. Immunol. Methods.* **1983**, 65, 55–63, https://doi.org/10.1016/0022-1759(83)90303-4
64. Mizutani, M.Y.; Takamatsu, Y.; Ichinose, T.; Nakamura, K.; Itai, A. Effective handling of induced-fit motion in flexible docking. *Proteins Struct. Funct. Bioinforma*. **2006**, 63, 878–891. https://doi.org/10.1002/prot.20931
65. Sharom, F.J. The P-glycoprotein efflux pump: How does it transport drugs?, *J. Membr. Biol.* **1997**, https://doi.org/10.1007/s002329900305
66. Lipinski, C.A. Lead- and drug-like compounds: the rule-of-five revolution. *Drug Discov. Today Technol*. **2004**, 1, 337–341, https://doi.org/10.1016/j.ddtec.2004.11.007 Vane JR, Botting RM. New insight into the mode of action of anti-inflammatory drugs. Inflamm Res (1995), 44:1–10, doi: 10.1007/BFO1630479
67. Lahuerta Zamora, L.; Perez-Gracia, M.T. Using digital photography to implement the McFarland method. *J. R. Soc. Interface* (*JRSICU).* **2012**, 9(73), 1892-7, https://doi.org/10.1098/rsif.2011.0809